

UNCLASSIFIED

AD NUMBER

ADB011428

LIMITATION CHANGES

TO:

Approved for public release; distribution is unlimited.

FROM:

Distribution authorized to U.S. Gov't. agencies only; Test and Evaluation; MAY 1976. Other requests shall be referred to Air Force Armament Laboratory, Eglin AIFB, FL 32542.

AUTHORITY

AFATL ltr, 10 Dec 1979

THIS PAGE IS UNCLASSIFIED

AEDC-TR-76-71
AFATL-TR-76-50

cy.2

JUN 11 1976
SEP 18 1990



SEPARATION CHARACTERISTICS OF THE MK-82 AIR WHEN RELEASED FROM THE F-111 AIRCRAFT AT MACH NUMBERS FROM 0.70 TO 1.25

PROPULSION WIND TUNNEL FACILITY
ARNOLD ENGINEERING DEVELOPMENT CENTER
AIR FORCE SYSTEMS COMMAND
ARNOLD AIR FORCE STATION, TENNESSEE 37389

May 1976

PROPERTY OF U.S. AIR FORCE
AEDC TECHNICAL LIBRARY

Final Report for Period 7 - 9 January 1976

Distribution limited to U.S. Government agencies only; this report contains information on test and evaluation of military hardware; May 1976; other requests for this document must be referred to Air Force Armament Laboratory (AFATL/DLJC), Eglin Air Force Base, Florida 32542

Prepared for

AIR FORCE ARMAMENT LABORATORY (DLJC)
EGLIN AIR FORCE BASE, FLORIDA 32542

NOTICES

When U. S. Government drawings specifications, or other data are used for any purpose other than a definitely related Government procurement operation, the Government thereby incurs no responsibility nor any obligation whatsoever, and the fact that the Government may have formulated, furnished, or in any way supplied the said drawings, specifications, or other data, is not to be regarded by implication or otherwise, or in any manner licensing the holder or any other person or corporation, or conveying any rights or permission to manufacture, use, or sell any patented invention that may in any way be related thereto.

Qualified users may obtain copies of this report from the Defense Documentation Center.

References to named commercial products in this report are not to be considered in any sense as an endorsement of the product by the United States Air Force or the Government.

APPROVAL STATEMENT

This technical report has been reviewed and is approved for publication.

FOR THE COMMANDER



JOHN C. CARDOSI
Lt Colonel, USAF
Chief Air Force Test Director, PWT
Directorate of Test



CRAIG E. MAHAFFY
Colonel, USAF
Director of Test

UNCLASSIFIED

DD FORM 1473 EDITION OF 1 NOV 65 IS OBSOLETE

UNCLASSIFIED

UNCLASSIFIED

20. ABSTRACT (Continued)

resulted in the store's passing very close to the underside of the F-111 wing.

UNCLASSIFIED

PREFACE

The work reported herein was conducted by the Arnold Engineering Development Center (AEDC), Air Force Systems Command (AFSC), at the request of the Air Force Armament Laboratory (AFATL/DLJC), under Program Element 64602F. The AFATL project monitor was Mr. Robert A. Hume. The results of the test were obtained by ARO, Inc. (a subsidiary of Sverdrup & Parcel and Associates, Inc.), contract operator of AEDC, AFSC, Arnold Air Force Station, Tennessee, under ARO Project Number P41C-B3A. The authors of this report were M. R. Cunningham and E. G. Allee, Jr., ARO, Inc. Data reduction was completed on January 16, 1976, and the manuscript (ARO Control No. ARO-PWT-TR-76-31) was submitted for publication on March 11, 1976.

CONTENTS

	<u>Page</u>
1.0 INTRODUCTION	5
2.0 APPARATUS	
2.1 Test Facility	5
2.2 Test Articles	6
2.3 Instrumentation	6
3.0 TEST DESCRIPTION	
3.1 Test Conditions	6
3.2 Data Acquisition	6
3.3 Corrections	7
3.4 Precision of Data	8
4.0 RESULTS AND DISCUSSION	8

ILLUSTRATIONS

Figure

1. Isometric Drawing of a Typical Store Separation Installation and a Block Diagram of the Computer Control Loop	11
2. Schematic of the Tunnel Test Section Showing Model Location	12
3. Sketch of the F-111 Aircraft Model	13
4. Details of the F-111 TAC Pivot Pylon and BRU-3A/A Multiple Rack	14
5. Dimensional Sketch of the MK-82 AIR Metric Store Model	15
6. Typical Tunnel Installation Photograph	16
7. Identification of the BRU-3A/A Store Stations	17
8. Configuration Identification	18
9. Effect of Wing Sweep Angle on the MK-82 AIR Trajectories	19
10. Trajectories Resulting from Release from Pylon 6, BRU Station 6 at $M_\infty = 1.15$	28
11. Effect of Varying the Ejector Force on the MK-82 AIR Trajectories from Pylon 6, BRU Station 6	29
12. Effect of Mach Number Variation on the MK-82 AIR Trajectories	30
13. Typical Effect of Altitude Variation on the MK-82 AIR Trajectories	36

TABLES

1. Wind Tunnel Nominal Test Conditions	38
2. Test Summary	39
3. Input Constants Used in Trajectory Calculations	44

NOMENCLATURE	46
------------------------	----

1.0 INTRODUCTION

A wind tunnel investigation was conducted in the Aerodynamic Wind Tunnel (4T) of the Propulsion Wind Tunnel Facility (PWT) to determine the separation characteristics of the MK-82 Air Inflatable Retarder (AIR) store from the F-111 aircraft. Trajectory data were acquired using a six-degree-of-freedom captive trajectory support (CTS) store separation system. All trajectories were initiated from BRU-3A/A racks attached to the F-111 aircraft at wing pylon stations 3 through 6. Data were obtained at Mach numbers from 0.7 to 1.25, aircraft angles of attack of 2 and 3 deg, wing leading-edge sweep angles from 45 to 72.5 deg, and simulated altitudes of 1,000 and 15,000 ft.

2.0 APPARATUS

2.1 TEST FACILITY

Tunnel 4T is a closed-loop, continuous flow variable density tunnel in which the Mach number can be varied from 0.1 to 1.3 and can be set at 1.6 and 2.0 by placing nozzle inserts over the permanent sonic nozzle. At all Mach numbers, the stagnation pressure can be varied from 300 to 3,700 psfa. The test section is 4 ft square and 12.5 ft long with perforated, variable porosity (0.5- to 10-percent open) walls. It is completely enclosed in a plenum chamber from which the air can be evacuated, allowing part of the tunnel airflow to be removed through the perforated walls of the test section.

For captive trajectory testing, two separate and independent support systems were used to support the models. The aircraft model was inverted in the test section and supported by an offset sting attached to the main pitch sector. The store model was supported by the CTS, which extends down from the tunnel top wall and provides store movement (six degrees of freedom) independent of the aircraft model. An isometric drawing of a typical installation is shown in Fig. 1.

Also shown in Fig. 1 is a block diagram of the computer control loop used during these tests. The analog system and the digital computer work as an integrated unit and, utilizing required input information, control the store movement. Positioning is accomplished by use of six individual d-c electric motors. Maximum translational travel of the CTS is ± 15 in. from the tunnel centerline in the lateral and vertical directions and 36 in. in the axial direction. Maximum angular displacements are ± 45 deg in pitch and yaw and ± 360 deg in roll. A schematic showing the test section details and the location of the models in the tunnel is shown in Fig. 2.

2.2 TEST ARTICLES

A sketch of the 0.0417-scale F-111 aircraft model is presented in Fig. 3. The model was geometrically similar to the full-scale airplane except that the tail section was removed to minimize interference with the CTS movement. The wing leading-edge sweep angle was variable and could be set at discrete angles of 26, 45, 54, 60, and 72.5 deg. The TAC pivot pylon and BRU-3A/A models (Fig. 4) were rotated to keep them parallel to the aircraft centerline at each wing sweep angle. Details of the 0.0417-scale MK-82 AIR store are presented in Fig. 5. The MK-82 AIR store is an MK-82GP store body modified with a BSU-49B tail section (air inflatable retarder, low drag housing). A typical tunnel installation photograph showing aircraft, store, and CTS is presented in Fig. 6.

2.3 INSTRUMENTATION

A four-component internal strain-gage balance was used to obtain store aerodynamic force and moment data. Translational and angular positions of the store were obtained from CTS analog inputs during the separation trajectories. The aircraft model angle of attack was determined using an internal, gravimetric angular position indicator. The pylons contained a touch wire system which enabled the store to be accurately positioned for launch. The system was also wired to automatically stop the CTS motion and give visual indication should the store or sting support make contact with any surface other than the touch wire.

3.0 TEST DESCRIPTION

3.1 TEST CONDITIONS

Wind tunnel nominal test conditions and a complete test summary are given in Tables 1 and 2. Store separation trajectory data were obtained at Mach numbers from 0.7 to 1.25. Tunnel conditions were held constant at the desired Mach number while the data were obtained. The captive trajectories were terminated when the store or sting contacted the aircraft model or when a CTS limit was reached.

3.2 DATA ACQUISITION

To obtain a trajectory, test conditions were established in the tunnel and the aircraft model was positioned at the desired angle of attack. Operational control of the CTS was then switched to the digital computer, which automatically oriented the store model at a position corresponding to the carriage location and then controlled the store movement during the trajectory through commands to the CTS analog system (see block diagram, Fig. 1). Data from the wind tunnel, consisting of measured model forces and moments,

wind tunnel operating conditions, and CTS rig positions, were input to the digital computer for use in the full-scale trajectory calculations.

The digital computer was programmed to solve the six-degree-of-freedom equations to calculate the angular and linear displacements of the store relative to the BRU-3A/A rack. In general, the program involves using the last two successive measured values of each static aerodynamic coefficient to predict the magnitude of the coefficients over the next time interval of the trajectory. These predicted values are used to calculate the new position and attitude of the store at the end of the time interval. The CTS is then commanded to move the store model to this new position, and the aerodynamic loads are measured. If these new measurements agree with the predicted values, the process is continued over another time interval of the same magnitude. If the measured and predicted values do not agree within the desired precision, the calculation is repeated over a time interval one-half the previous value. This process is repeated until a complete trajectory has been obtained.

In applying the wind tunnel data to the calculations of the full-scale store trajectories, the measured forces and moments are reduced to coefficient form and then applied with proper full-scale store dimensions and flight dynamic pressure. Dynamic pressure was calculated using a flight velocity equal to the free-stream velocity component plus the components of store velocity relative to the aircraft, and a density corresponding to the simulated altitude.

The initial portion of each launch trajectory incorporated simulated ejector forces in addition to the measured aerodynamic forces acting on the store. The ejector force was considered to act perpendicular to the BRU-3A/A rack mounting surface. The ejector forces and locations, along with other full-scale parameters used in the trajectory calculations, are listed in Table 3. The various BRU-3A/A weapons stations and the aircraft configurations are identified in Figs. 7 and 8.

3.3 CORRECTIONS

Balance, sting, and support deflections caused by the aerodynamic loads on the store models were accounted for in the data reduction program to calculate the true store-model angles. Corrections were also made for model weight tares to calculate the net aerodynamic forces on the store model.

Since no axial-force measurement was made on the store model, axial-force coefficients were estimated from data obtained during previous test programs. The values used are listed in Table 3c. These values were utilized as constants throughout each trajectory calculation.

3.4 PRECISION OF DATA

The trajectory data are subject to error from several sources including tunnel conditions, balance measurements, extrapolation tolerances allowed in the predicted coefficients, computer inputs, and CTS positioning control. Extrapolation tolerances were ± 0.10 for the aerodynamic coefficients. The maximum uncertainties in the full-scale position data caused by the balance inaccuracies are given below:

M_∞	t, sec	Uncertainties			
		ΔY , ft	ΔZ , ft	$\Delta \theta$, deg	$\Delta \psi$, deg
0.7	0.4	± 0.11	± 0.1	± 0.4	± 0.5
0.8				± 0.4	± 0.5
0.9				± 0.6	± 0.7
0.95				± 0.7	± 0.8
0.97				± 0.7	± 0.8
1.02				± 0.7	± 0.8
1.05				± 0.9	± 1.0
1.15				± 1.1	± 1.1
1.25				± 1.1	± 1.3

4.0 RESULTS AND DISCUSSION

Captive trajectory data obtained on the MK-82 AIR are presented in Figs. 9 through 13 as functions of full-scale trajectory time with both angular and linear displacements given relative to the flight-axis system. Positive X, Y, and Z displacements are forward, to the right, and down as seen by the pilot. Positive changes in θ , ψ , and ϕ from a view looking upstream are nose up, nose right, and clockwise roll, respectively. A trajectory was terminated when a CTS travel limit was reached, when the store or CTS rig contacted some part of the aircraft or its support structure, or upon determination that the store had cleared the aircraft. A complete listing of the trajectories which were obtained is given in Table 2. However, only those data which show significant trends are presented in this report. Unless otherwise noted, all launches were at a simulated altitude of 1,000 ft and had forward and aft ejector forces of 1,000 and 800 lb, respectively.

The effects of the wing sweep angle on store separation are presented in Fig. 9 for various Mach numbers and store release stations. At $M_\infty = 0.7$, the effect of changing the wing sweep angle was negligible (see Figs. 9a and b). As Mach number was increased, an increase in wing sweep angle usually resulted in a decrease in the magnitude of the

pitch and yaw excursions of the store. This effect varied with the pylon and rack stations from which the trajectory was initiated (see Figs. 9c through i).

At $M_\infty = 1.05$ for wing sweep angles of 54 and 60 deg, stores released from the forward inboard stations of racks mounted on pylons 3 and 6 exhibited an initial movement inboard and then reversed direction and moved outboard. However, at a sweep angle of 72.5 deg, the store continued inboard toward the centerline of the aircraft model. As Mach number was increased to $M_\infty = 1.25$, stores released from these inboard stations at the 72.5-deg wing sweep also reversed their initial motion in the Y direction and moved back outboard (see Figs. 9f through i).

During the test no store contact with the aircraft was experienced after store release; however, launches of the MK-82 Air from BRU-3A/A station 6 on pylon 6 at $M_\infty = 1.15$ separated in a manner which resulted in the stores passing in close proximity to the aircraft wing. After release, the store "floated" back upward under the wing until it attained a Z-position slightly closer to the aircraft than the initial release point. At the point closest to the aircraft, the store was pitched nose down approximately 10 deg (see Fig. 10). Ejector forces were changed to apply an 1,800-lb force at the forward ejector location. This ejector force did increase the minimum distance between the store and the aircraft wing. However, the general characteristics of the trajectory motion were the same (see Fig. 11).

The effect of Mach number variation on the separation characteristics of the MK-82 AIR are shown in Fig. 12 for a wing sweep angle of 54 deg. The major variations in the trajectories were noted in the pitching and yawing motions of the store. The magnitude and direction of motions varied with the pylon station and BRU-3A/A station from which release was initiated.

A few trajectories were obtained at simulated altitudes of both 1,000 and 15,000 ft. Typical results are shown in Fig. 13. No major changes in motion of the store were seen as a result of altitude variation.

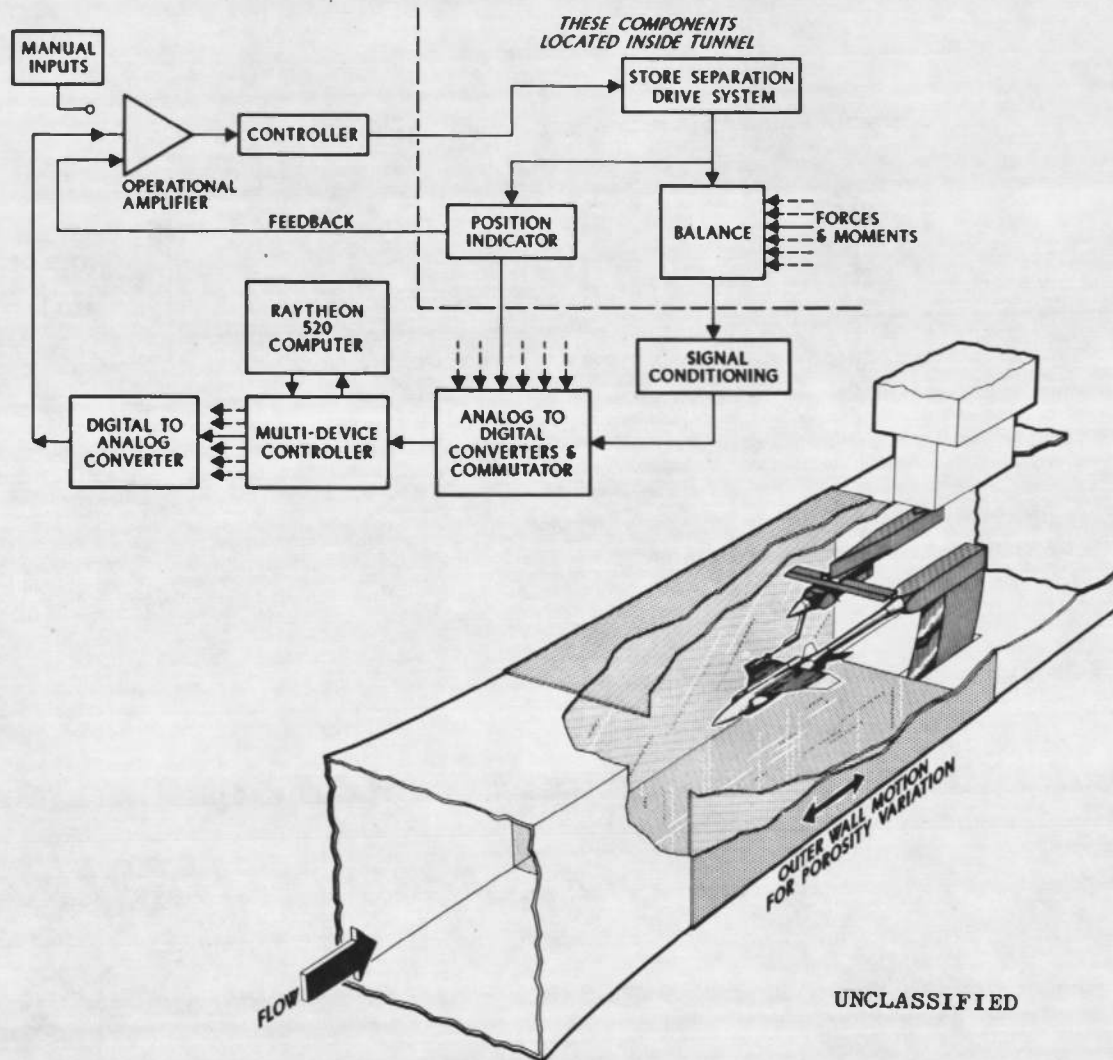
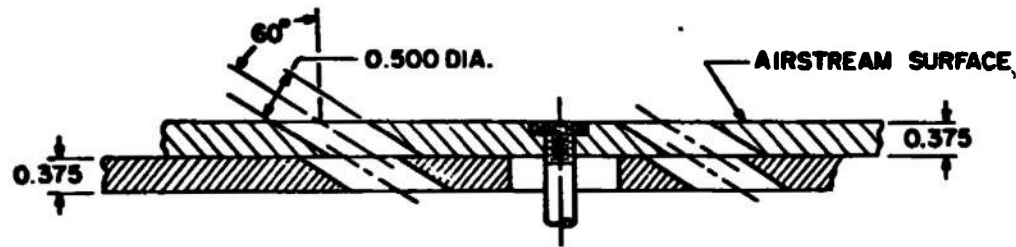


Figure 1. Isometric drawing of a typical store separation installation and a block diagram of the computer control loop.



TYPICAL PERFORATED WALL CROSS SECTION

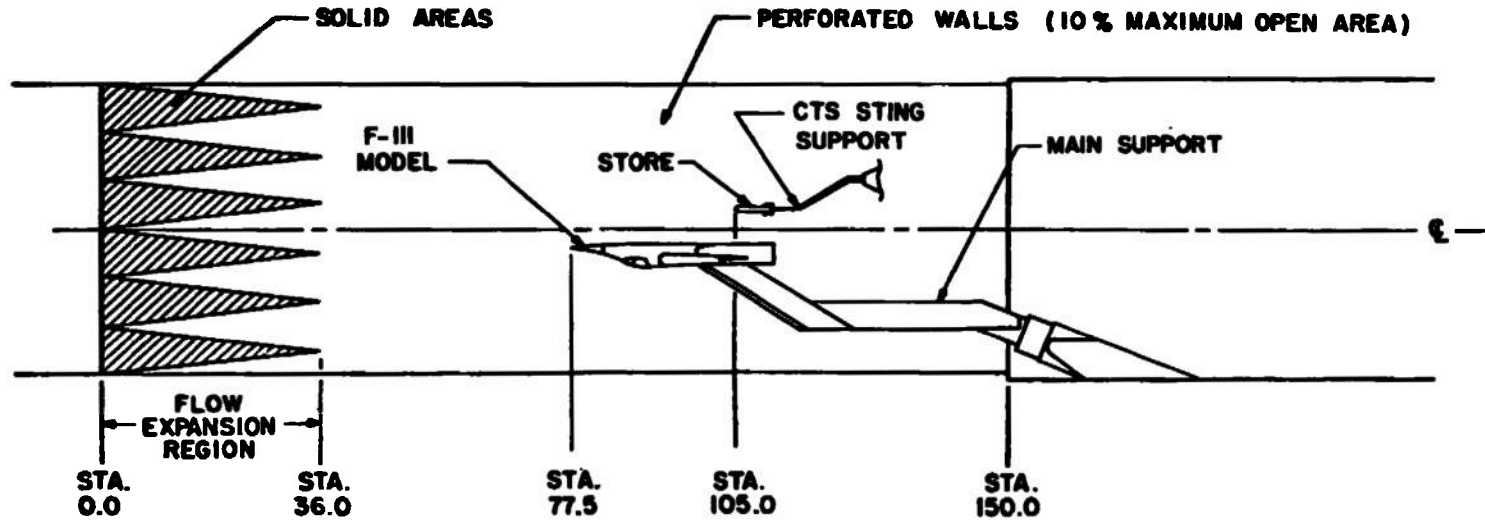
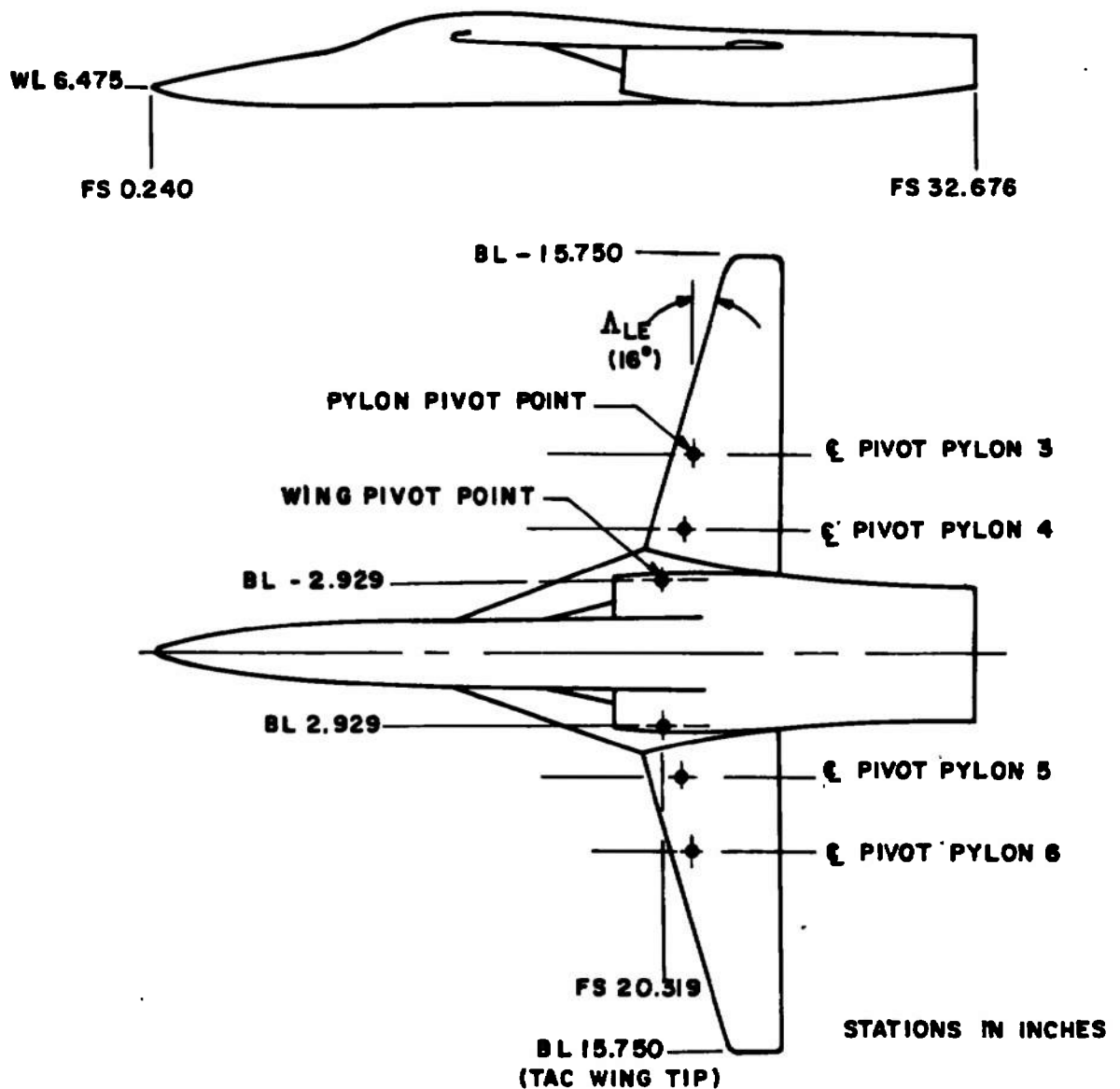
TUNNEL STATIONS AND
DIMENSIONS IN INCHES

Figure 2. Schematic of the tunnel test section showing model location.



Δ_{LE}	INBD PYLON PIVOT POINT		OUTBD PYLON PIVOT POINT	
	FS	BL	FS	BL
16 (Ref)	20.962	4.913	21.291	7.873
26	21.297	4.771	22.135	7.629
45	21.843	4.352	23.566	6.782
54	22.047	4.096	24.129	6.226
60	22.160	3.910	24.452	5.810
72.5	22.238	3.488	24.978	4.847

Figure 3. Sketch of the F-111 aircraft model.

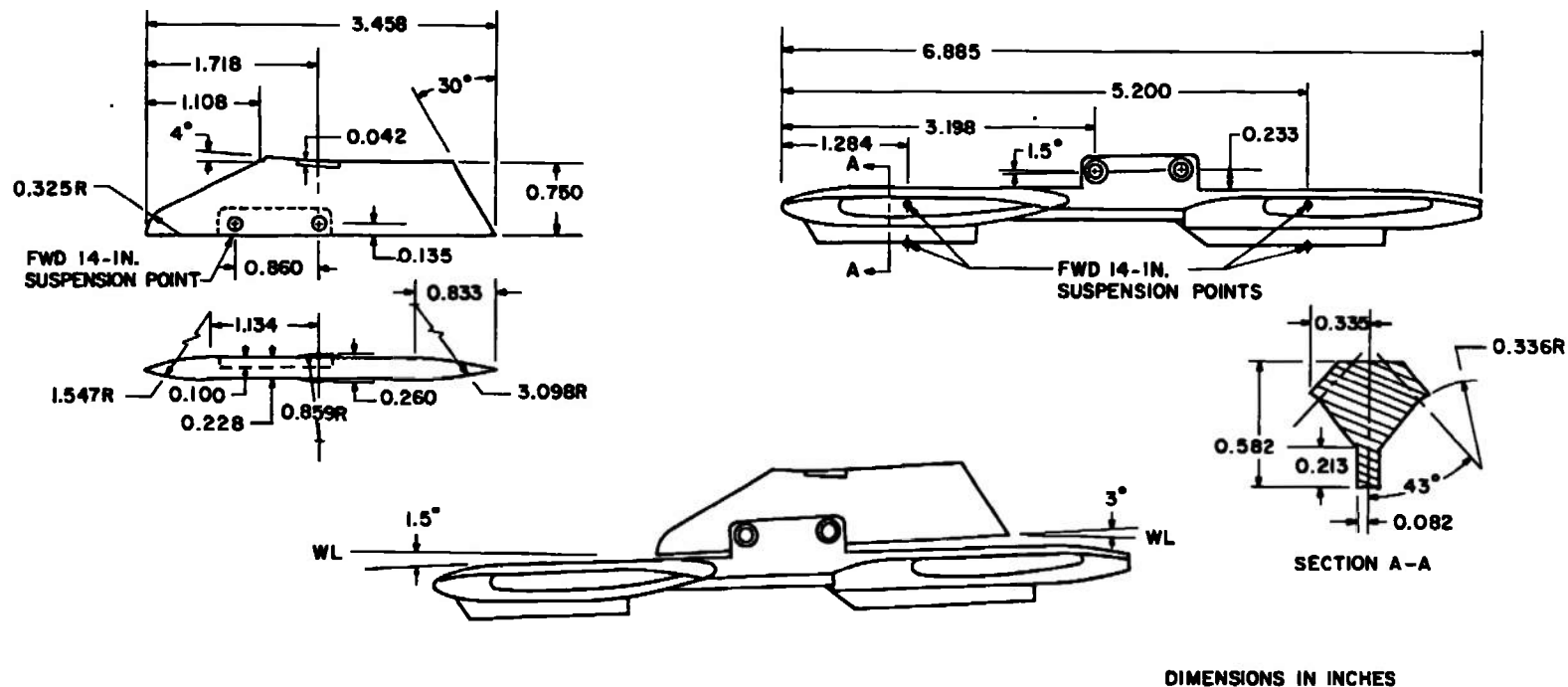


Figure 4. Details of the F-111 TAC pivot pylon and BRU-3A/A multiple rack.

STA	DIAM
0.000	0.000
0.221	0.193
0.229	0.197
0.297	0.233
0.314	0.242
0.357	0.261
0.400	0.278
0.485	0.308
0.570	0.333
0.656	0.355
0.741	0.373
0.826	0.390
0.912	0.405
0.997	0.418
1.082	0.430

STA	DIAM
1.168	0.439
1.253	0.446
1.338	0.448
1.893	0.448
1.978	0.447
2.063	0.444
2.149	0.439
2.234	0.432
2.319	0.423
2.405	0.412
2.490	0.400
2.575	0.387
2.661	0.371
2.689	0.366

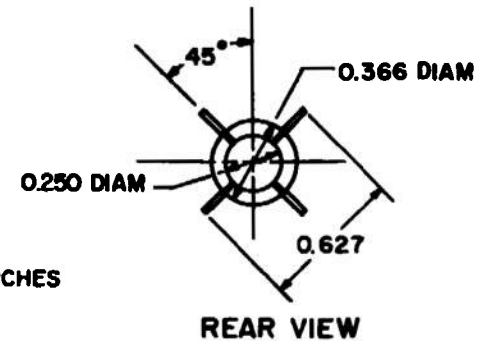
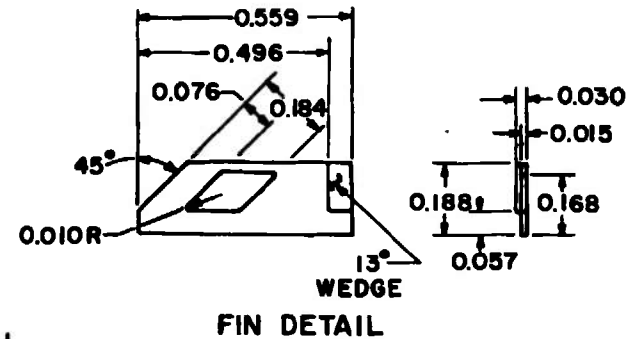
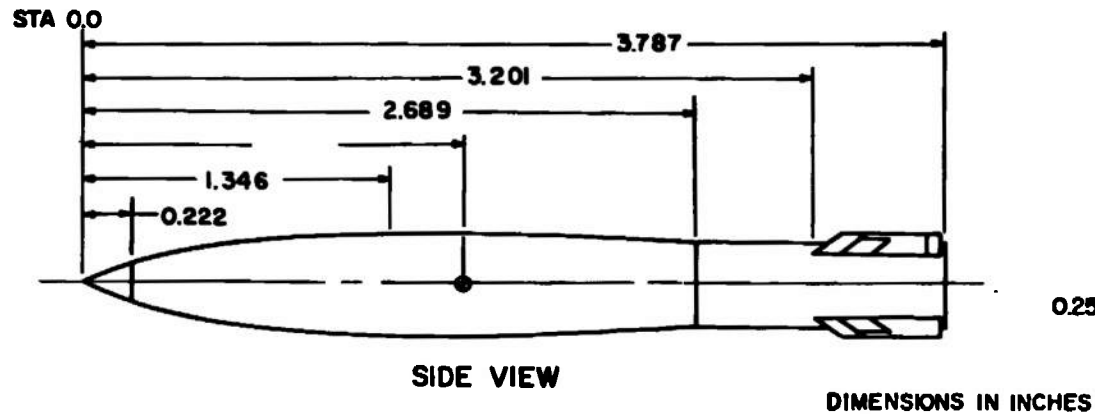


Figure 5. Dimensional sketch of the MK-82 AIR metric store model.

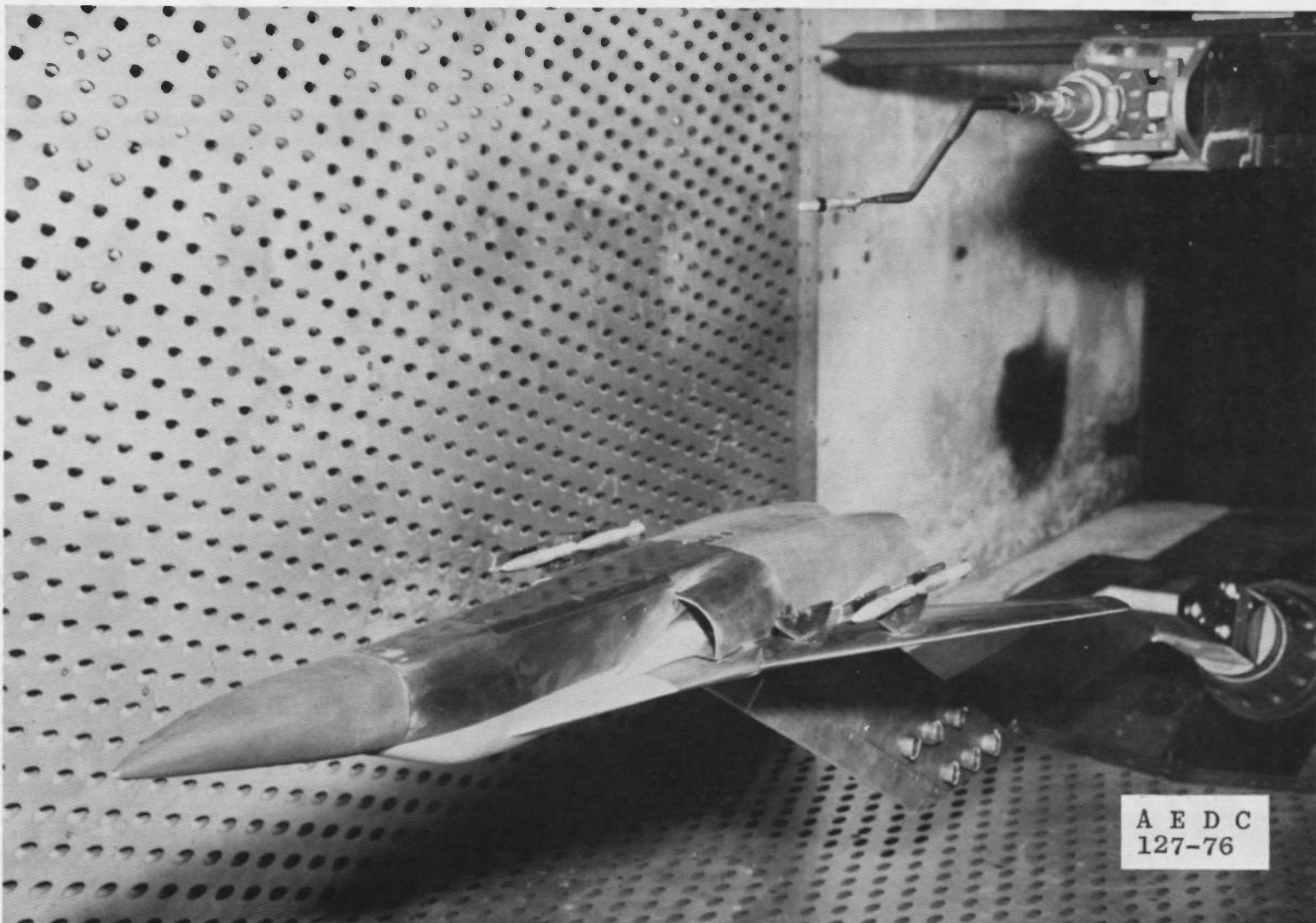
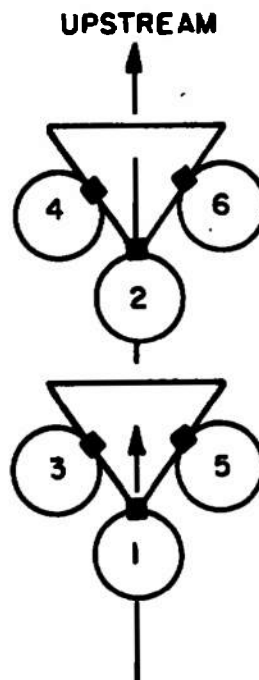


Figure 6. Typical tunnel installation photograph.



NOTE: The square indicates the orientation of the suspension lugs

TYPE RACK	STATION	ROLL ORIENTATION, deg
BRU-3A/A ↓	1	0
	2	0
	3	43
	4	43
	5	-43
	6	-43

Figure 7. Identification of the BRU-3A/A store stations.

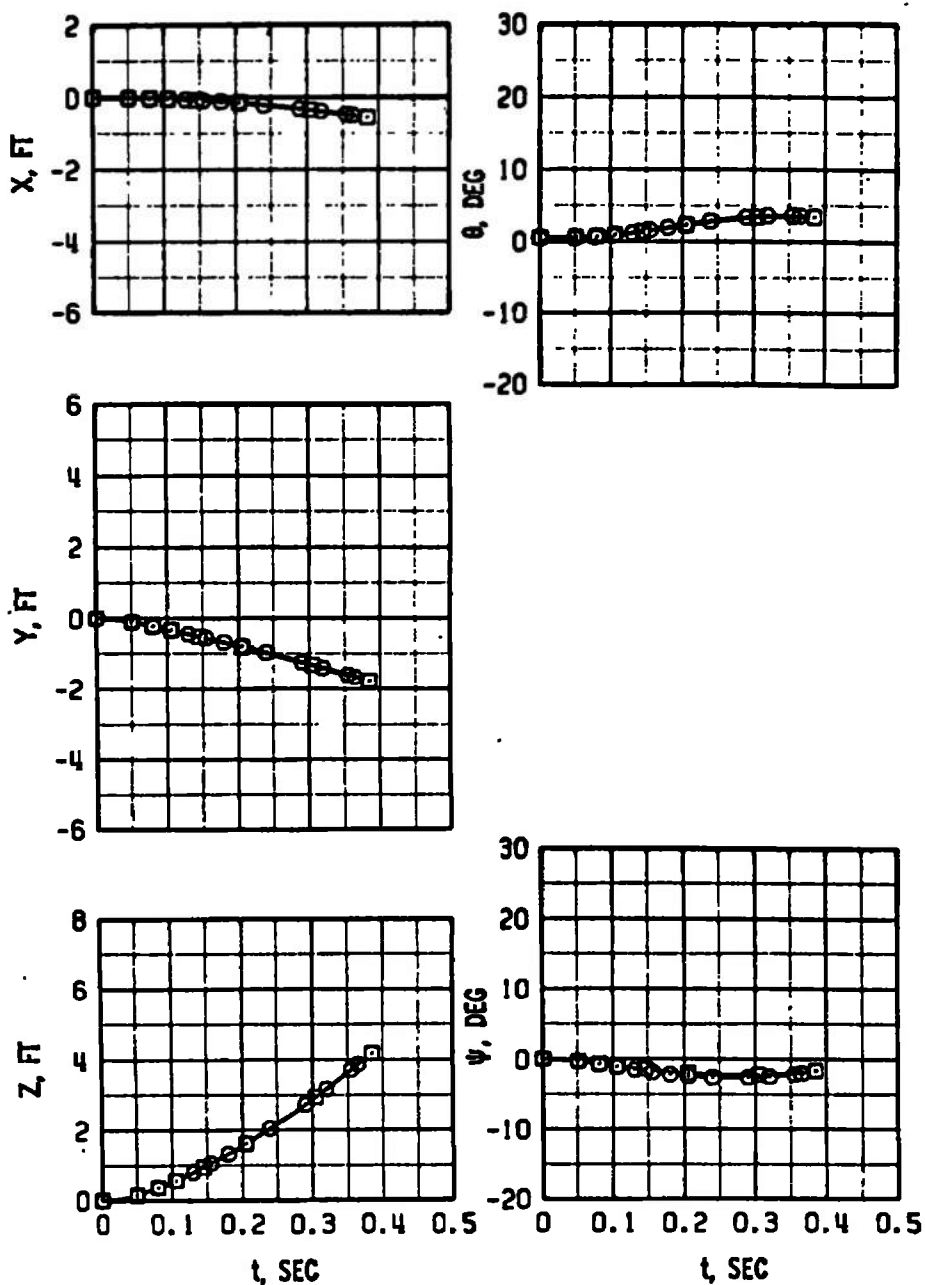
Config	Metric Store Fin Orientation	F-111 Aircraft Fuselage									
		Looking Upstream		Left Wing		Fuselage		Right Wing			
		Pylon No.									
		①	②	③	④	⑤	⑥	⑦	⑧		
1		Clean	Clean						Clean	Clean	
2											
3					Empty		Empty				
4											
5											
6							Empty				
7											
8					Empty						
9											
10											
11											

○ Denotes dummy store
 ● Denotes metric store
 Clean - Denotes pylon removed
 Empty - Denotes no store on pylon

Fwd }
 Aft } Denotes BRU-3 A/A rack

Figure 8. Configuration identification.

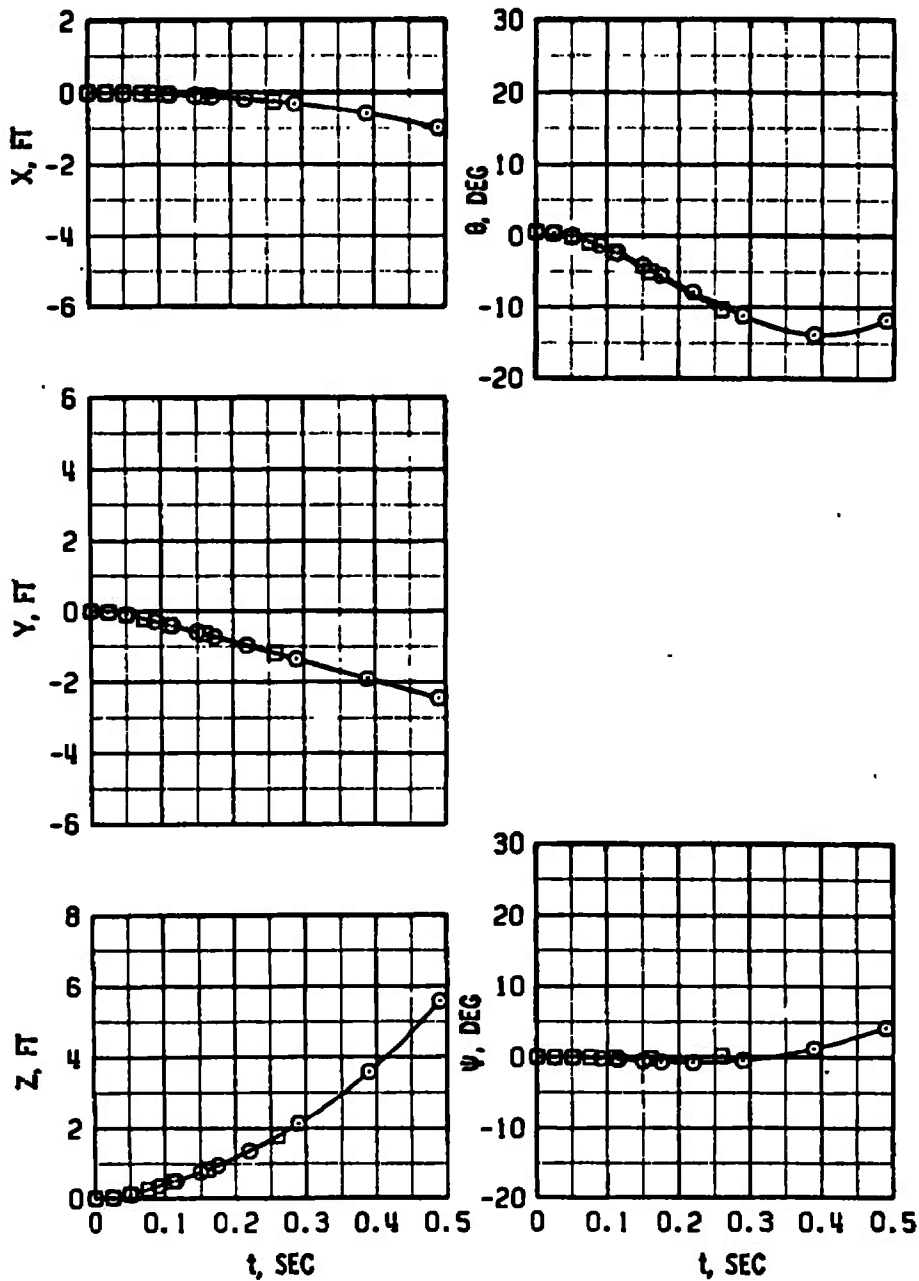
SYM	M_∞	α	Λ_x	PYLON	BAU	STA	CONF
○	0.70	2	45	3	4	2	
□	0.70	2	54	3	4	2	



a. $M_\infty = 0.70$, configuration 2, pylon 3

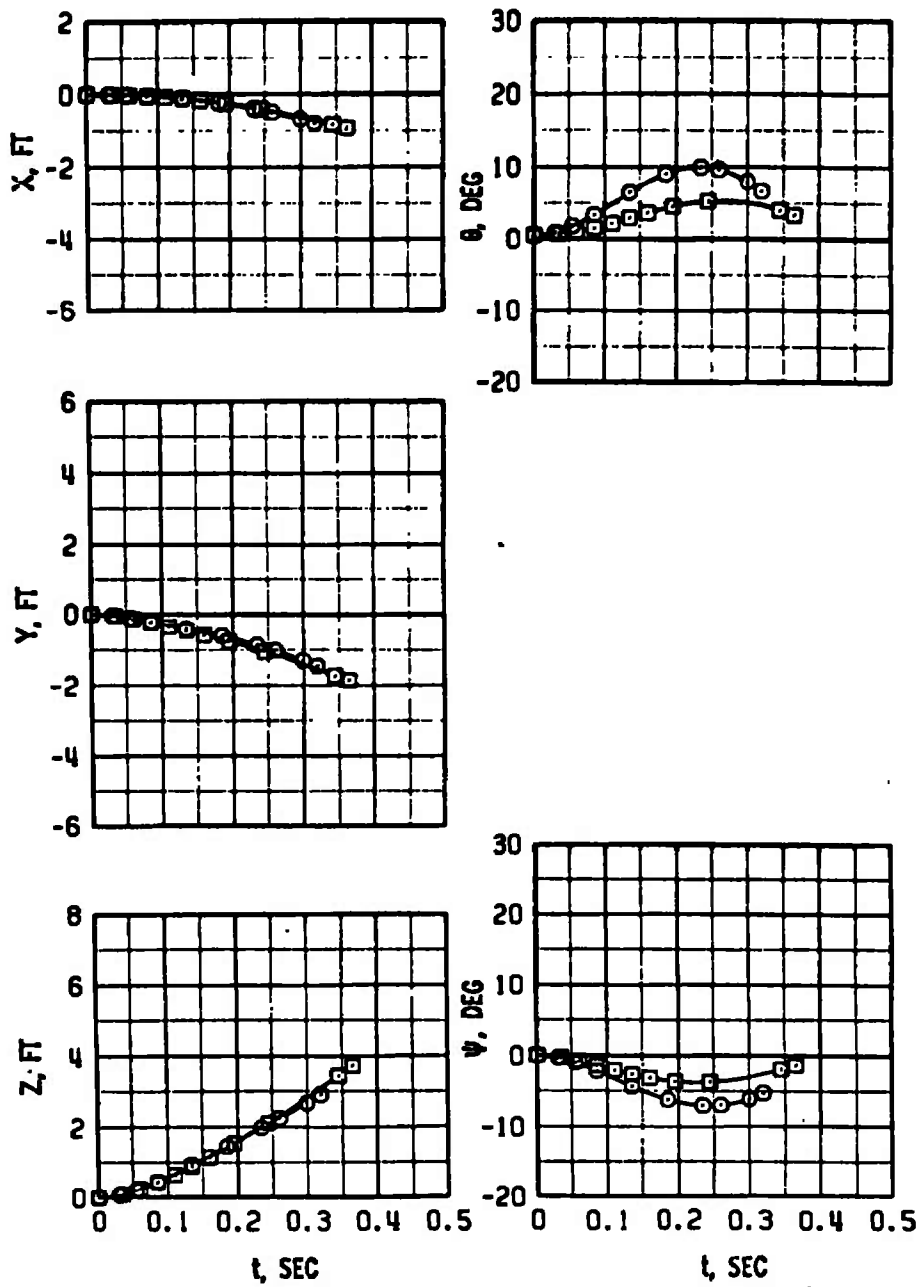
Figure 9. Effect of wing sweep angle on the MK-82 AIR trajectories.

SYM	M_∞	α	Λ_{LE}	PYLON	BRU	STA	CONF
○	0.70	2	45	5	3	2	
□	0.70	2	54	5	3	2	



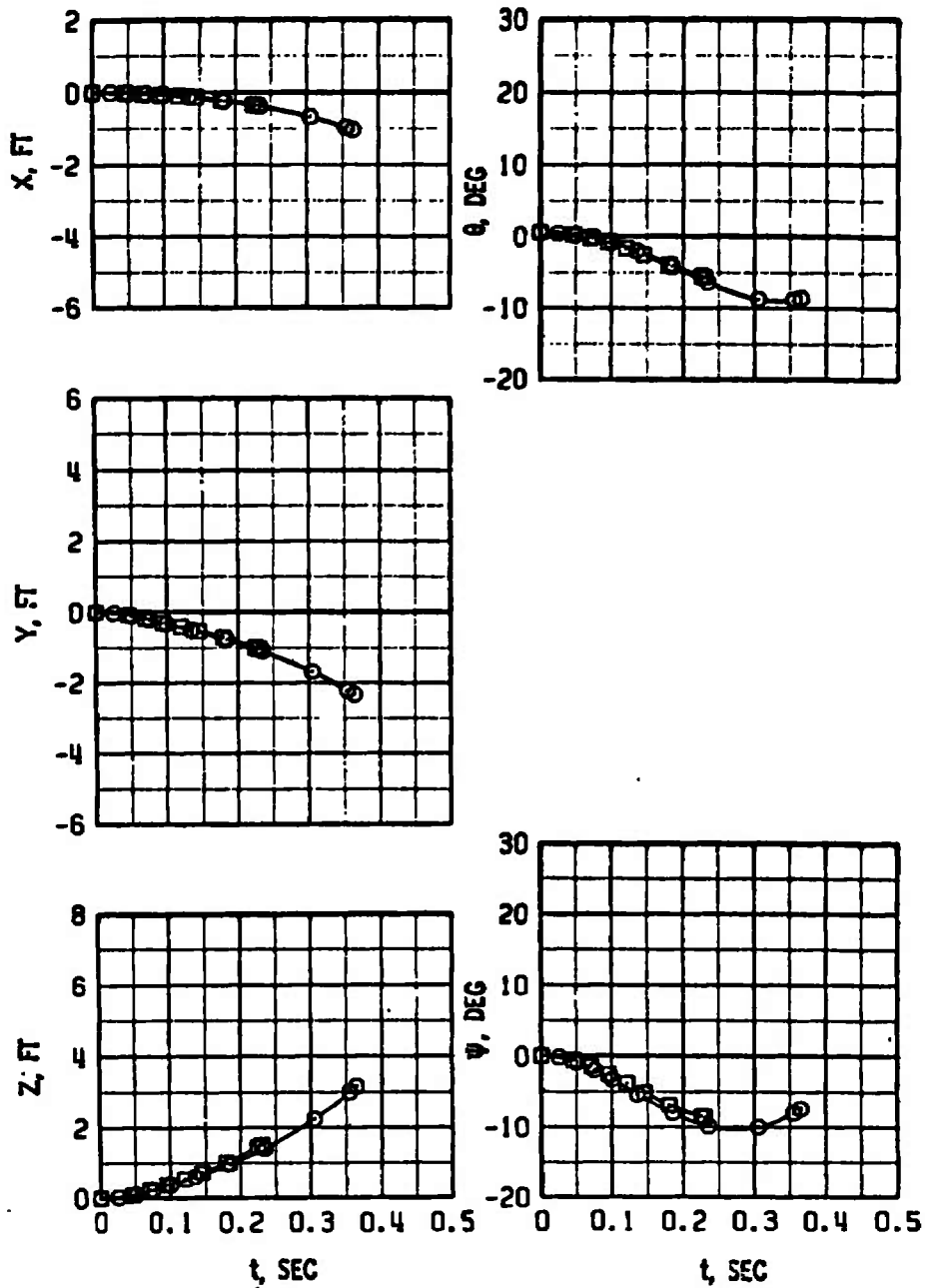
b. $M_\infty = 0.70$, configuration 2, pylon 5
Figure 9. Continued.

SYM	M_∞	α	Λ_{LE}	PYLON	BAU	STA	CONF
○	0.90	2	45	3	4	2	
□	0.90	2	54	3	4	2	



c. $M_\infty = 0.90$, configuration 2, pylon 3
Figure 9. Continued.

SYM	M_∞	α	A_{LE}	PYLON	BRU	STA	CONF
○	0.90	2	45	6	3	2	
□	0.90	2	54	6	3	2	



d. $M_\infty = 0.90$, configuration 2, pylon 6
Figure 9. Continued.

SYM	M_∞	α	Λ_{LE}	PYLON	BRU	STA	CONF
○	1.05	2	54	3	5	10	
□	1.05	2	60	3	5	10	
△	1.05	3	72.5	3	5	10	

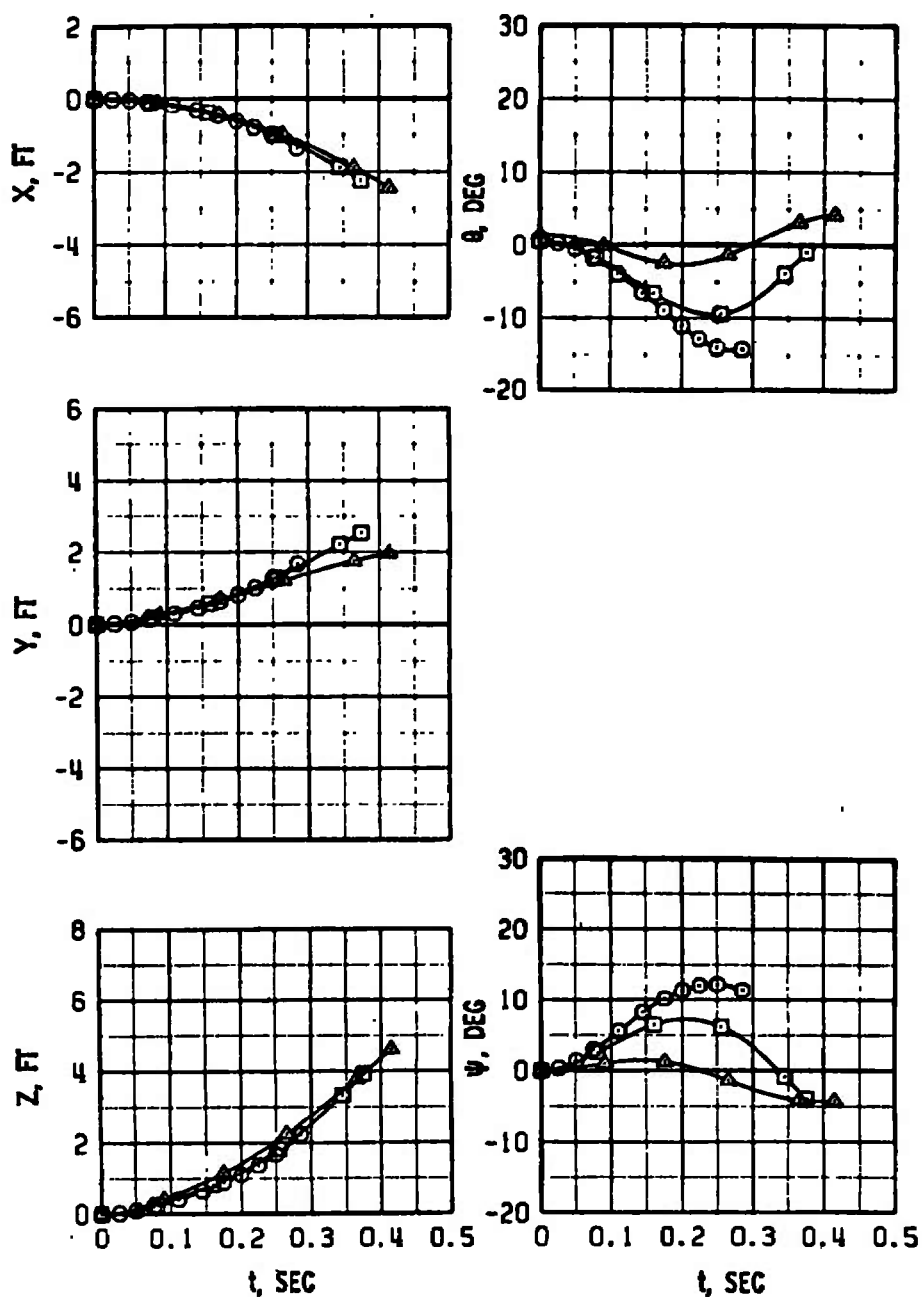
e. $M_\infty = 1.05$, configuration 10, pylon 3

Figure 9. Continued.

SYM	M_∞	α	Λ_{LE}	PYLON	BRU STA	CONF
○	1.05	2	54	3	6	11
□	1.05	2	60	3	6	11
△	1.05	3	72.5	3	6	11

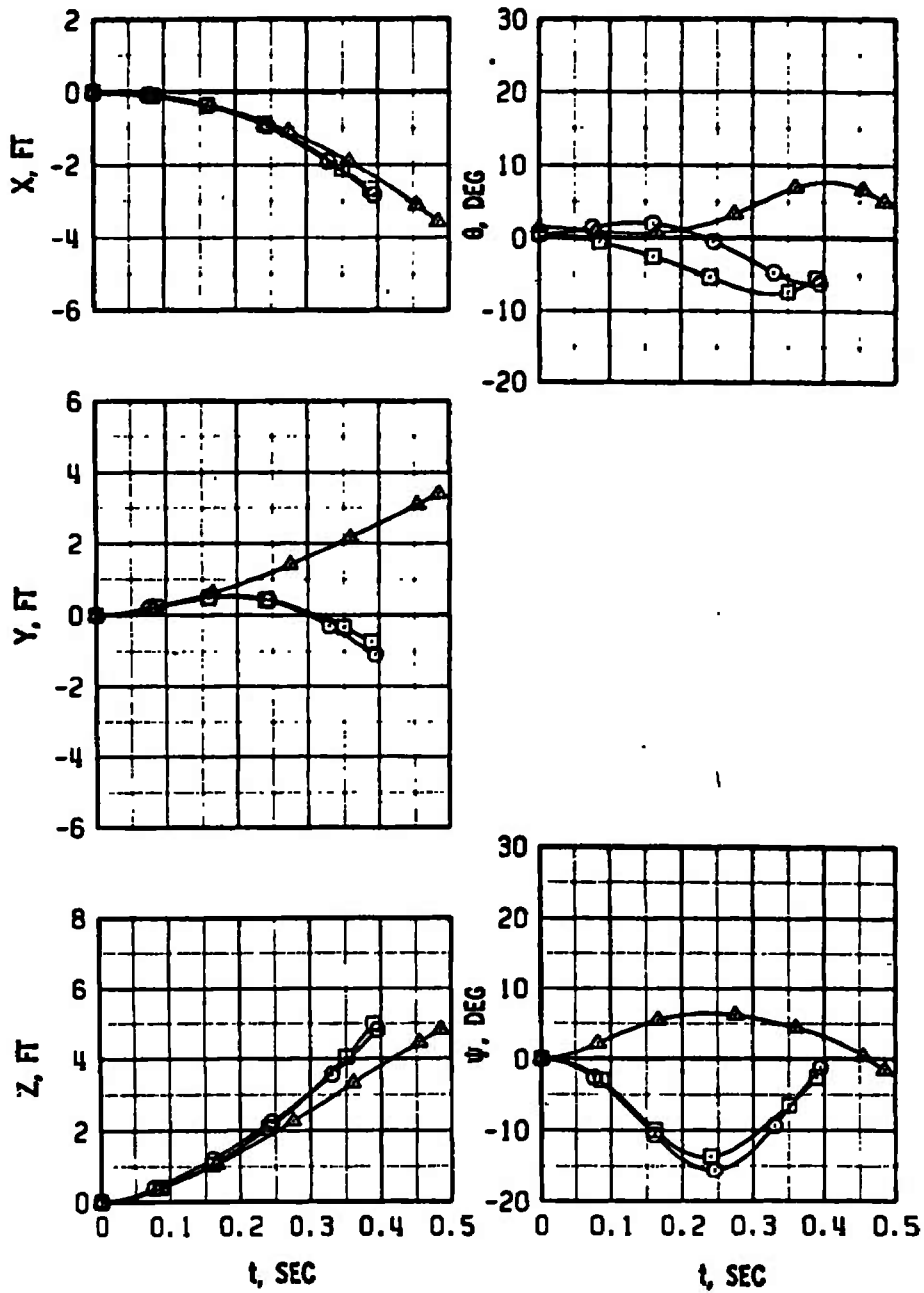
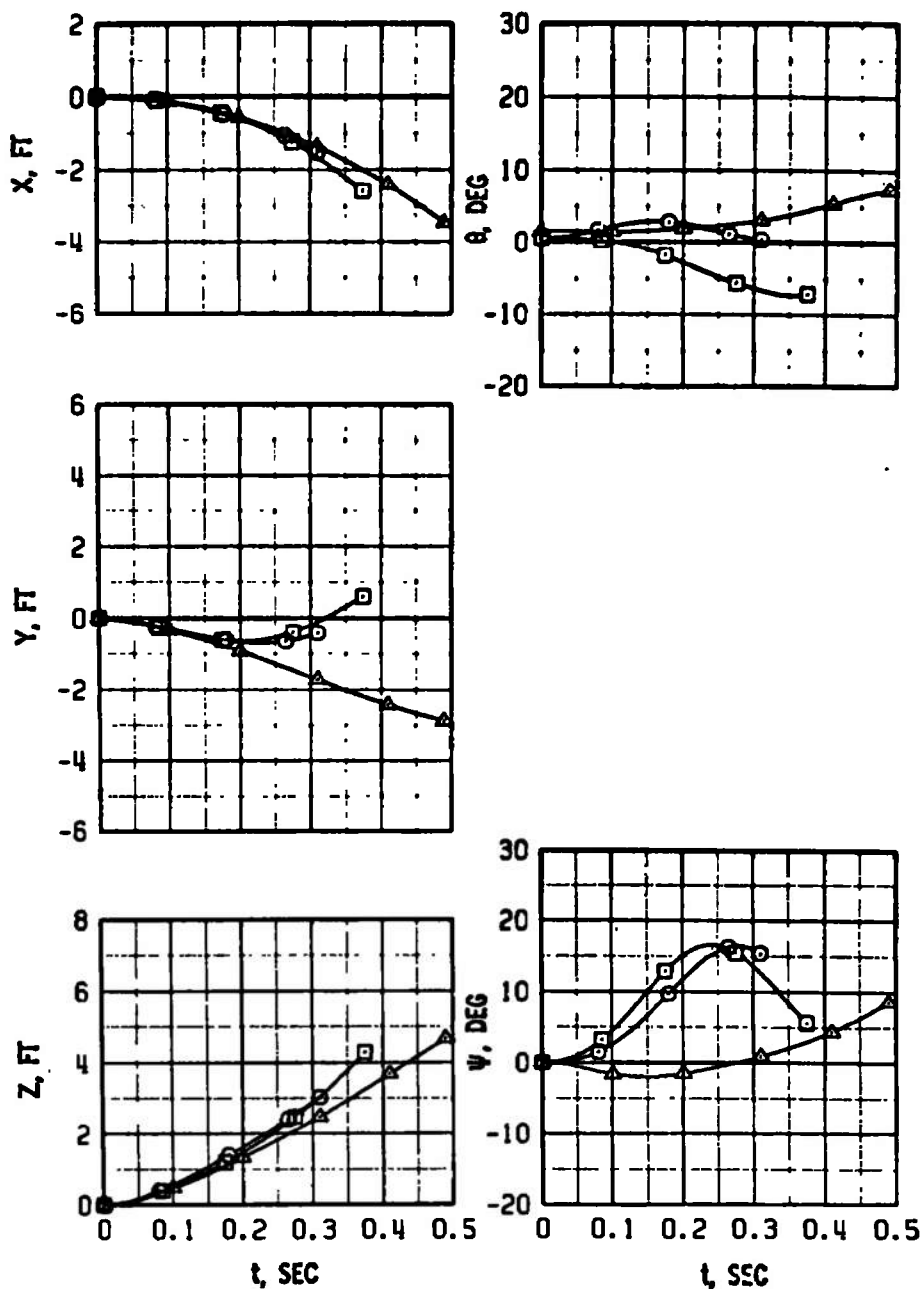
f. $M_\infty = 1.05$, configuration 11, pylon 3

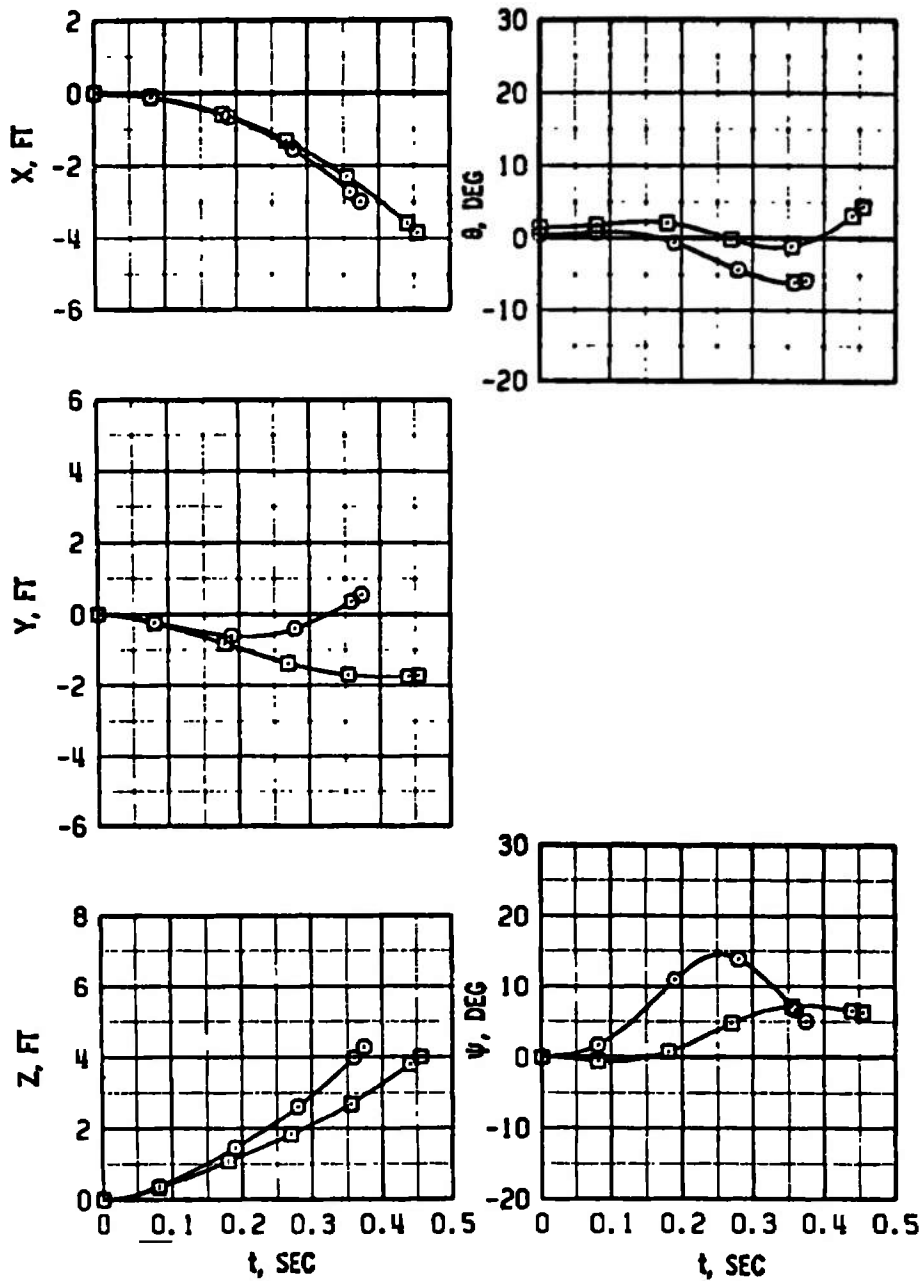
Figure 9. Continued.

SYM	M_∞	α	A_{t1}	PYLON	BRU	STA	CONF
○	1.05	2	54	6	4	11	
□	1.05	2	60	6	4	11	
△	1.05	3	72.5	6	4	11	



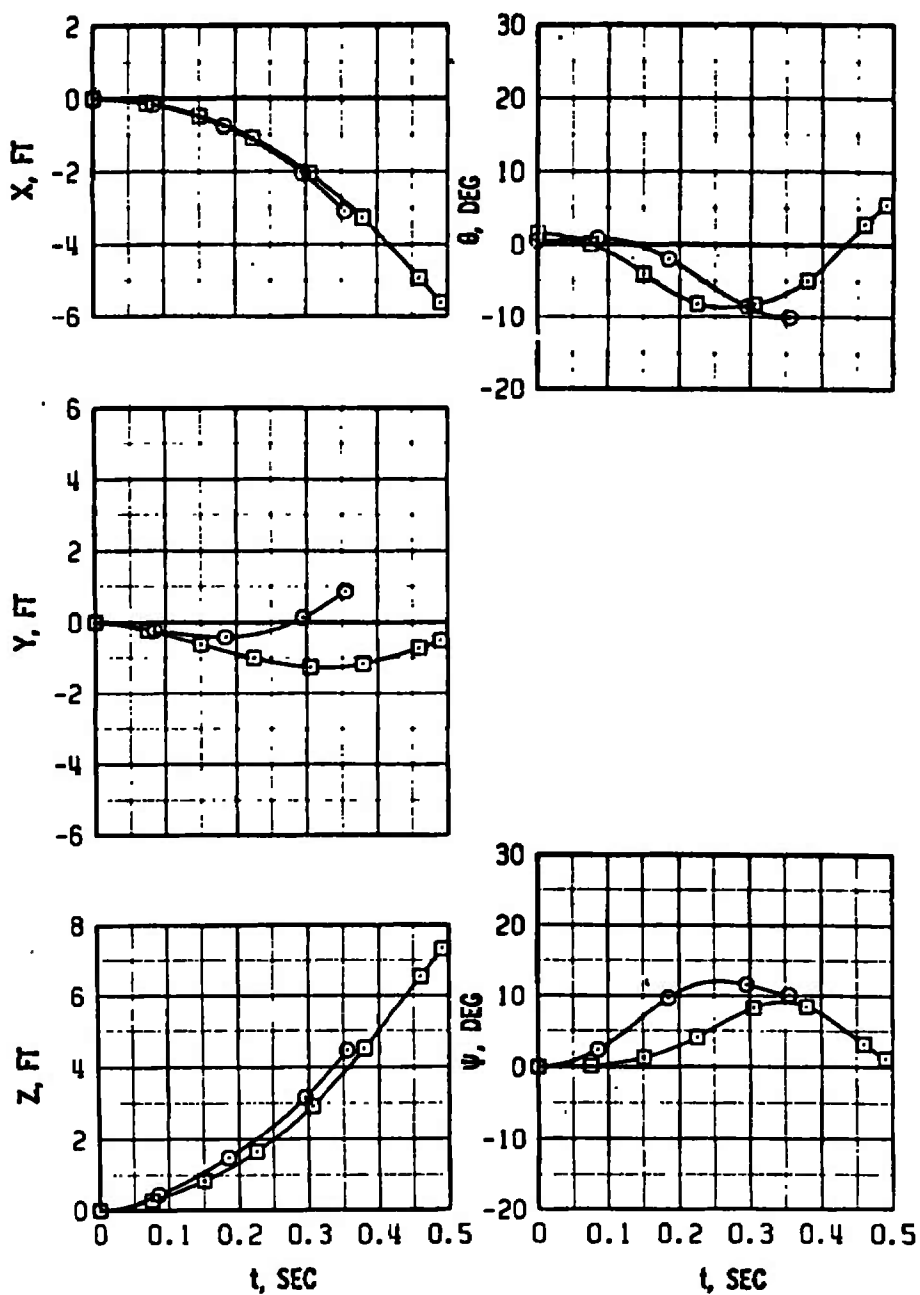
g. $M_\infty = 1.05$, configuration 11, pylon 6
Figure 9. Continued.

SYM	M_∞	α	Λ_L	PYLON	BRU STA	CONF
○	1.15	2	60	6	4	11
□	1.15	3	72.5	6	4	11



h. $M_\infty = 1.15$, configuration 11, pylon 6
Figure 9. Continued.

SYM	M_∞	α	A_{LE}	PYLON	BRU	STR	CONF
○	1.25	2	60	6	4	11	
□	1.25	3	72.5	6	4	11	



i. $M_\infty = 1.25$, configuration 11, pylon 6
Figure 9. Concluded.

SYM	M_∞	α	A_{LE}	PYLON	BRU STA	CONF
○	1.15	2	60	6	6	9
□	1.15	3	72.5	6	6	9

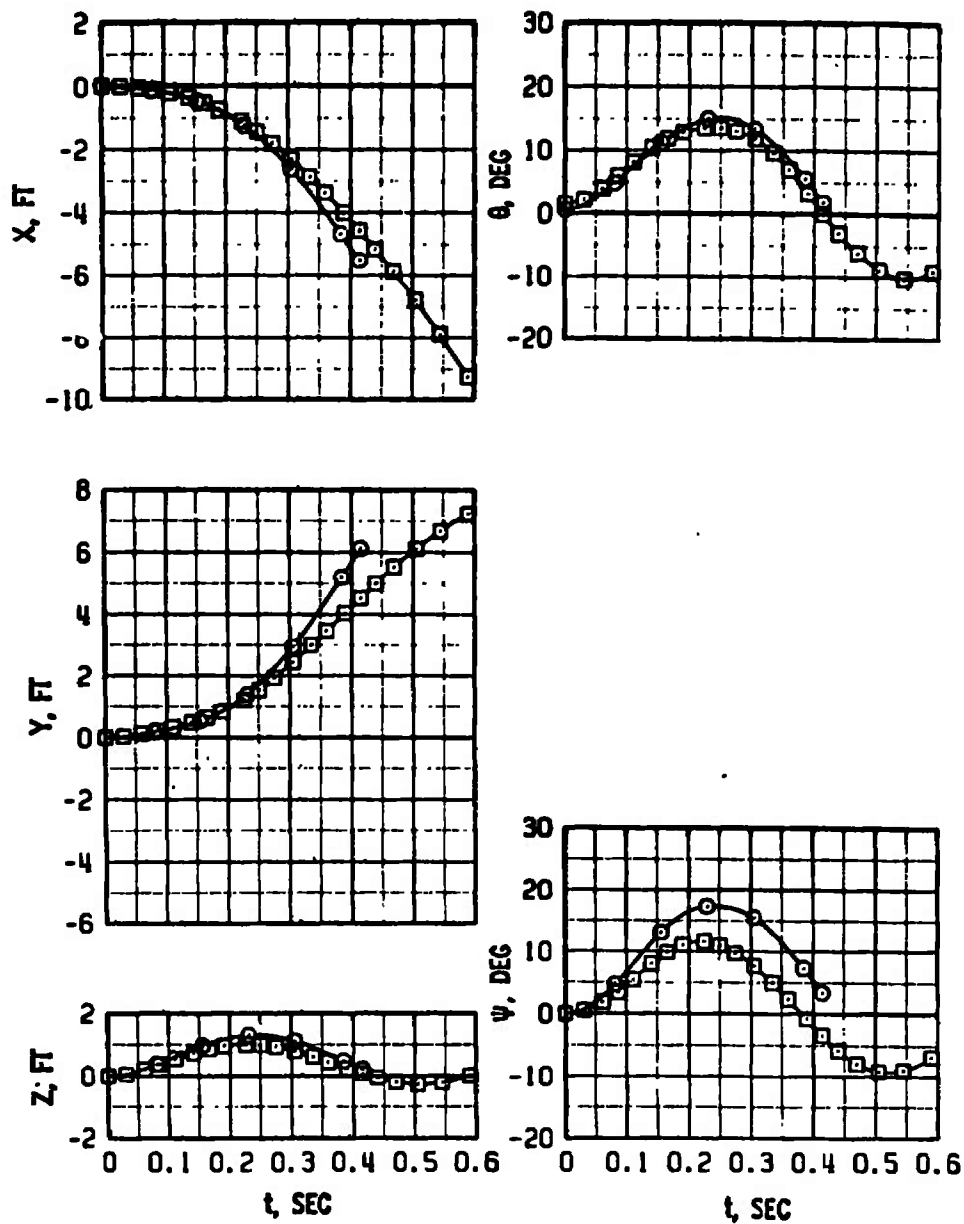


Figure 10. Trajectories resulting from release from pylon 6, BRU station 6 at $M_\infty = 1.15$.

SYM	M_L	α	Λ_{LE}	PYLON	BRU STA	CONF	F_{Z1}	F_{Z2}
○	1.15	3	72.5	6	6	9	1,000	800
△	1.15	3	72.5	6	6	9	1,800	0

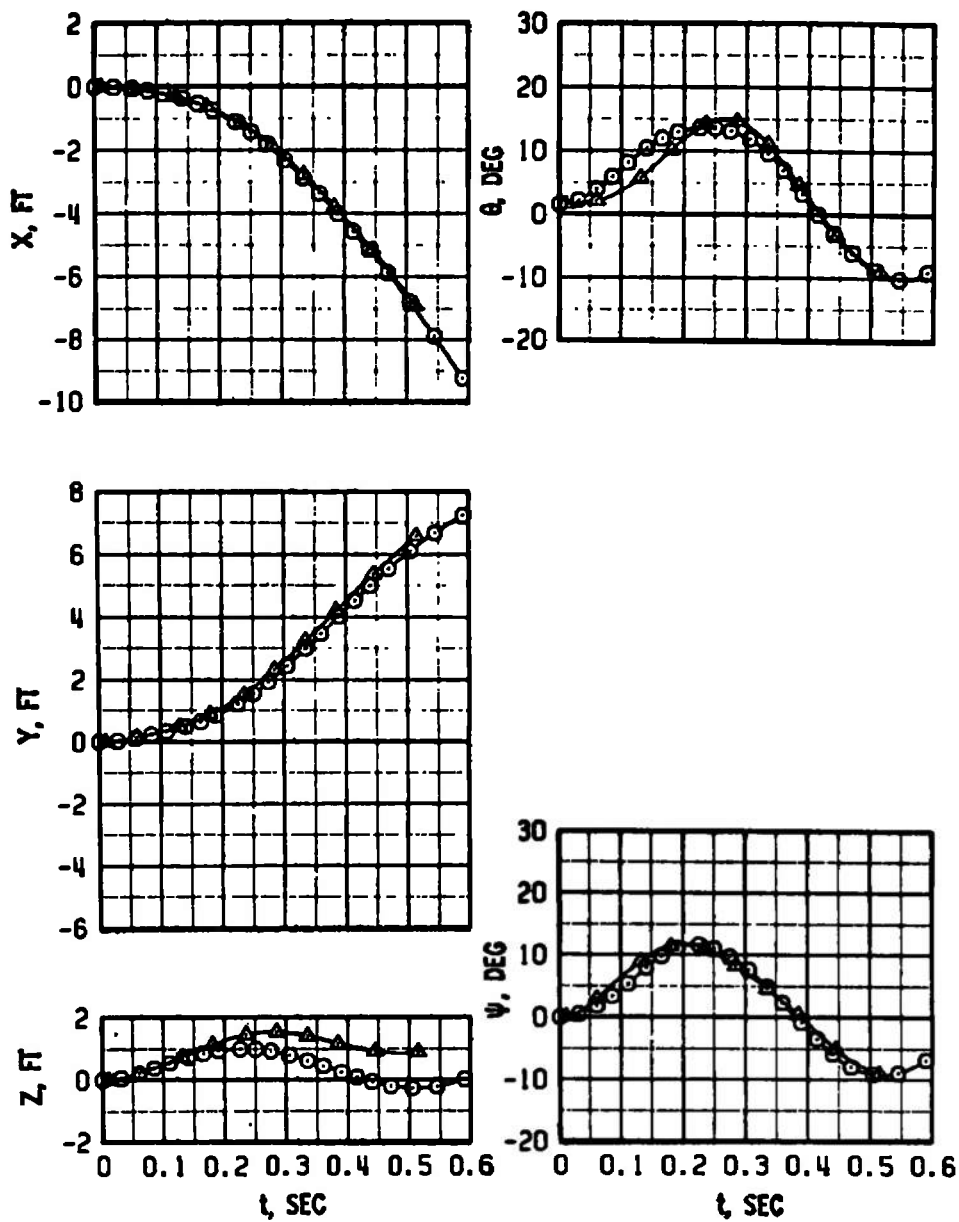
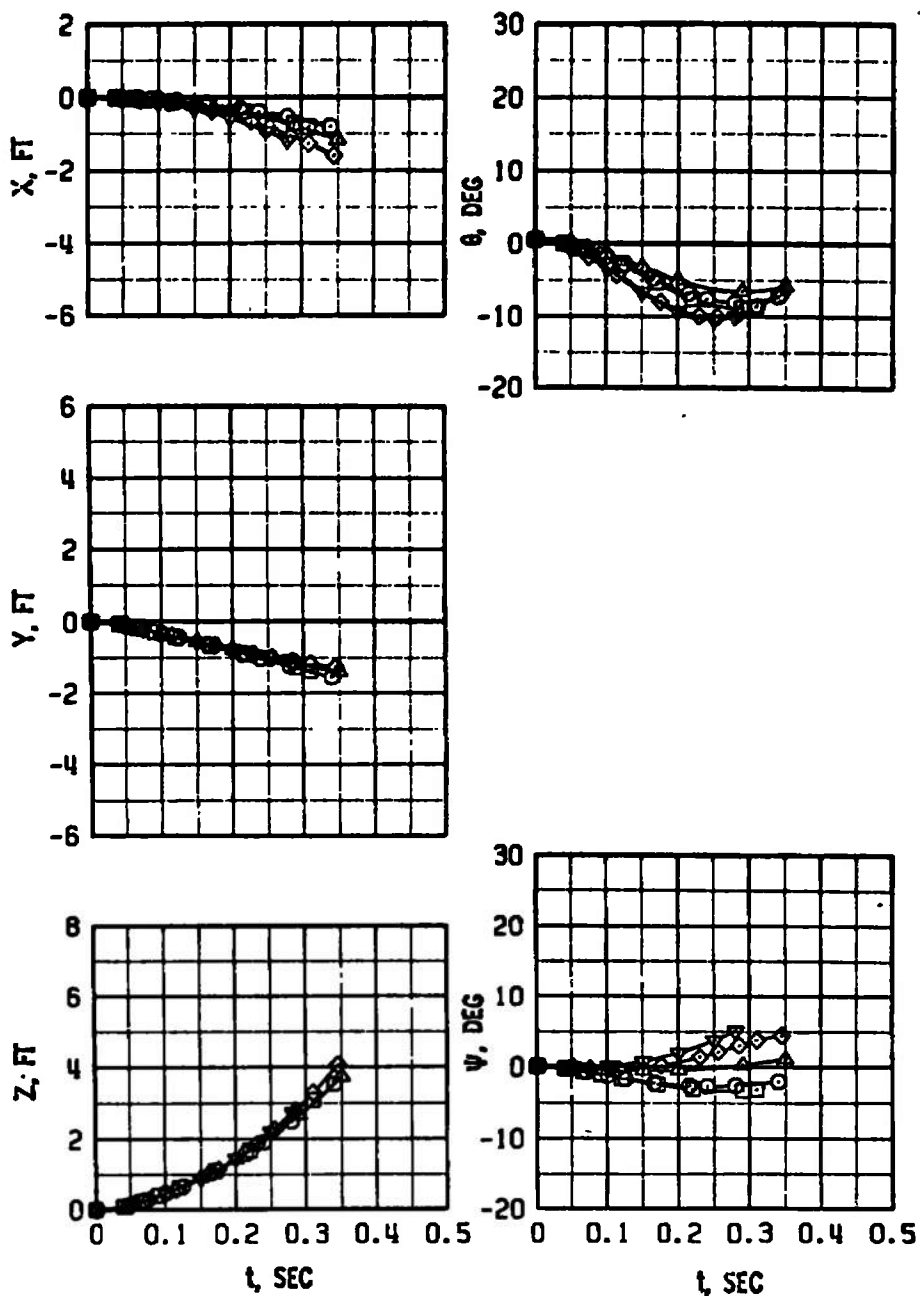


Figure 11. Effect of varying the ejector force on the MK-82 AIR trajectories from pylon 6, BRU station 6.

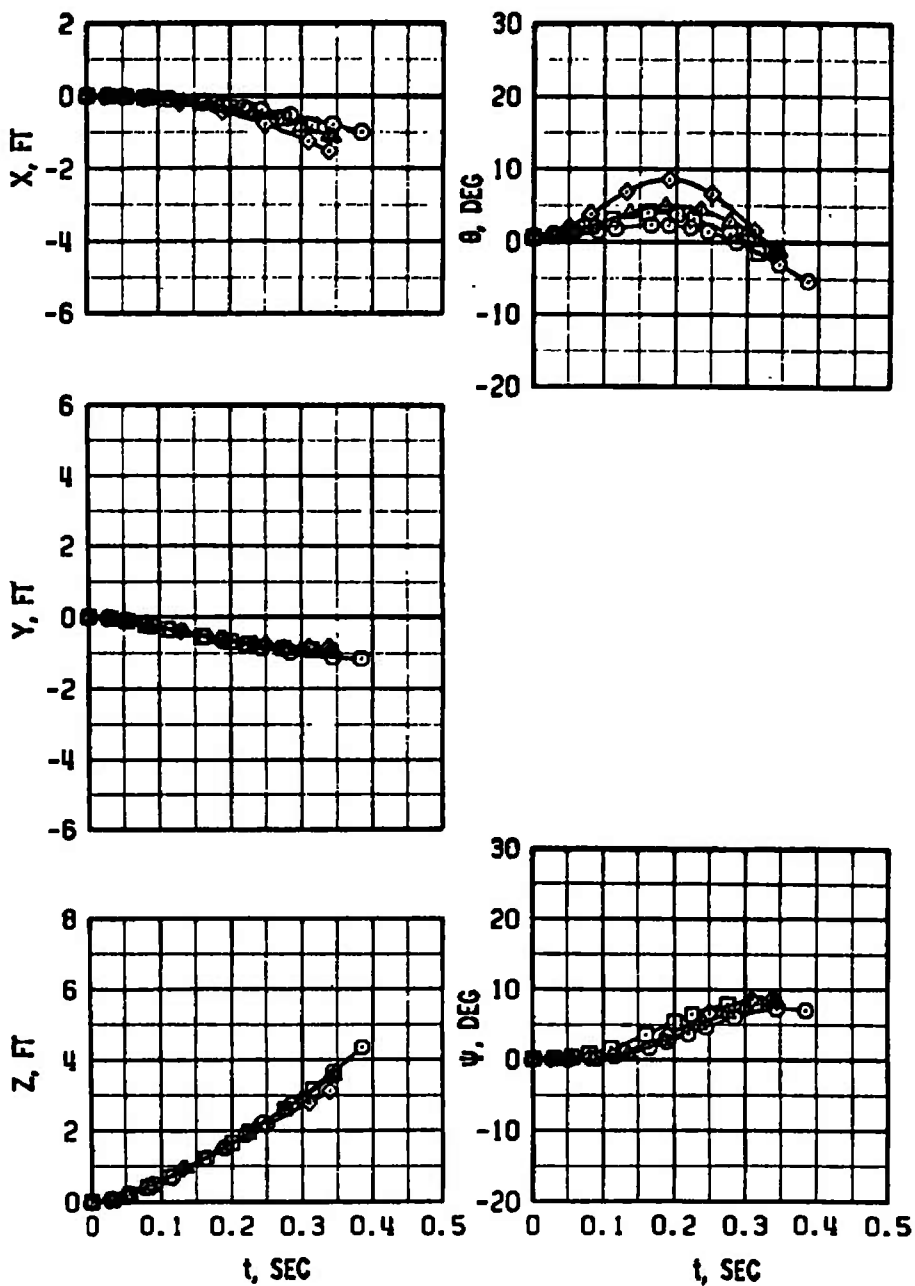
SYM	M _∞	α	A _{LZ}	PYLON	BRU	STR	CONF
○	0.90	2	54	3	3	4	
□	0.95	2	54	3	3	4	
△	0.97	2	54	3	3	4	
◇	1.02	2	54	3	3	4	
▽	1.05	2	54	3	3	4	



a. Configuration 4, pylon 3

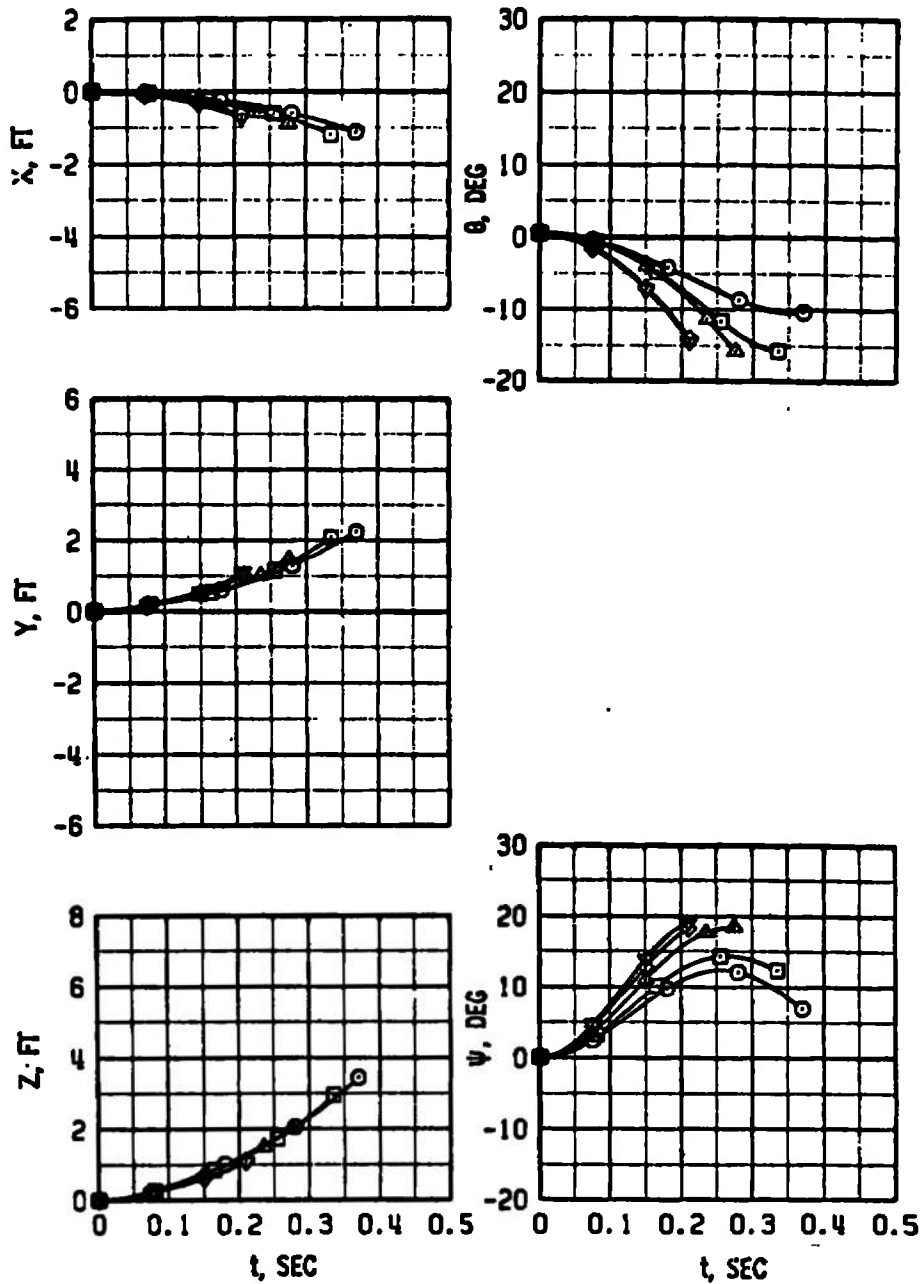
Figure 12. Effect of Mach number variation on the MK-82 AIR trajectories.

SYM	M_∞	α	A_{LE}	PYLON	BAU	STR	CONF
○	0.90	2	54	6	4	4	4
□	0.95	2	54	6	4	4	4
▲	0.97	2	54	6	4	4	4
◇	1.02	2	54	6	4	4	4



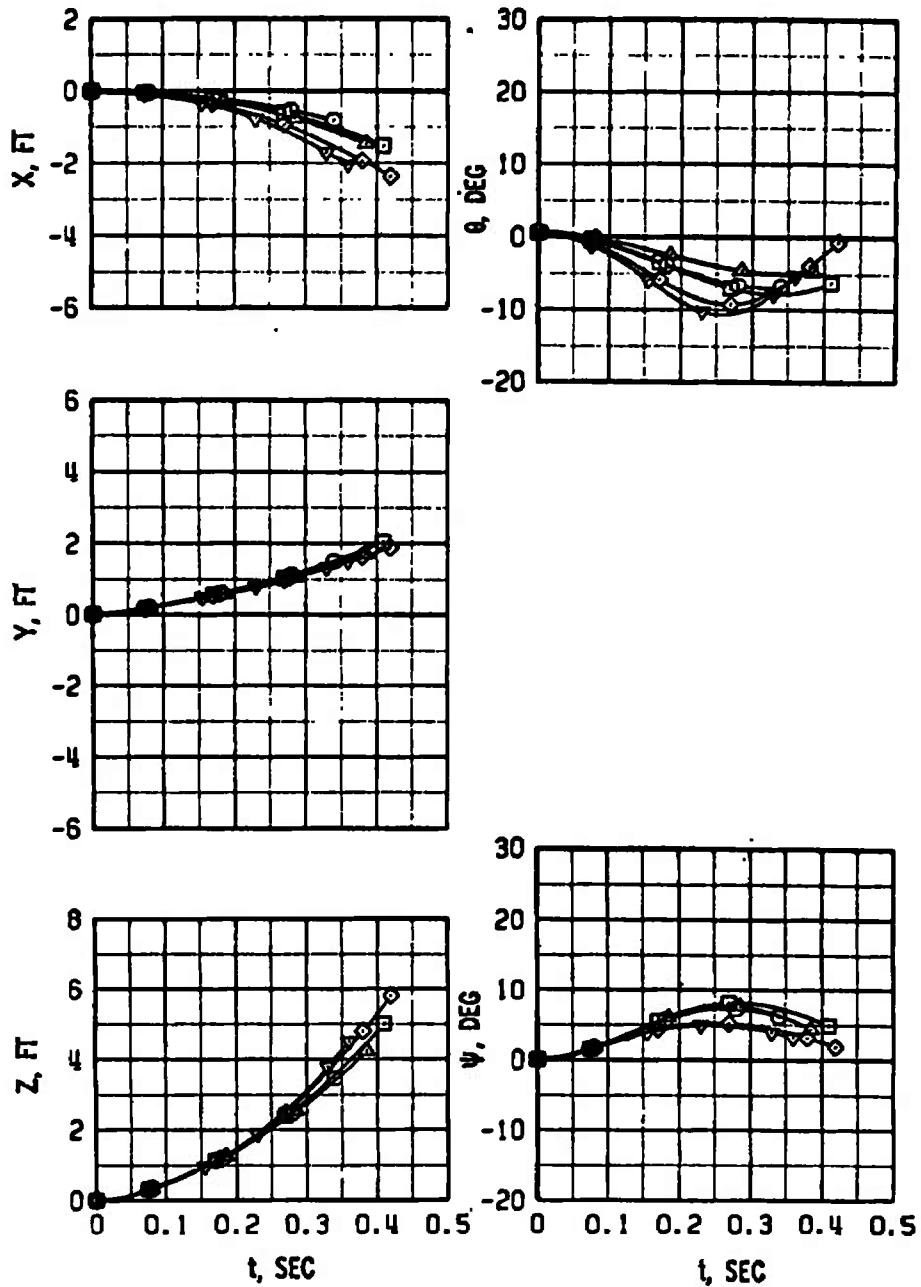
b. Configuration 4, pylon 6
Figure 12. Continued.

SYM	M _L	α	Λ_{LE}	PYLON	BRU	STA	CONF
○	0.90	2	54	3	5	6	
□	0.95	2	54	3	5	6	
△	0.97	2	54	3	5	6	
◇	1.02	2	54	3	5	6	
▽	1.05	2	54	3	5	6	



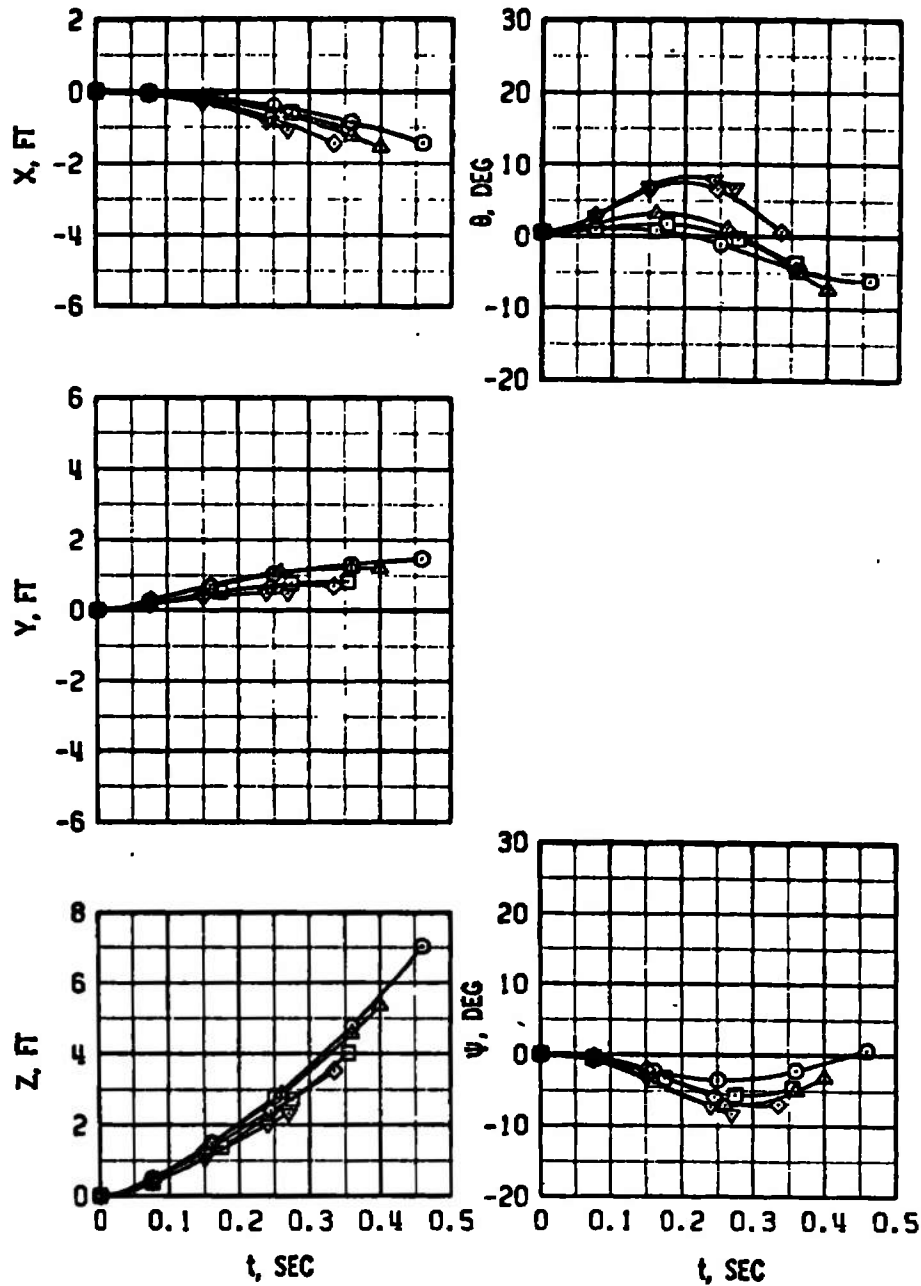
c. Configuration 6, pylon 3
Figure 12. Continued.

SYM	M_∞	α	A_{LE}	PYLON	BAU STA	CONF
○	0.90	2	54	6	5	6
□	0.95	2	54	6	5	6
▲	0.97	2	54	6	5	6
◇	1.02	2	54	6	5	6
▽	1.05	2	54	6	5	6



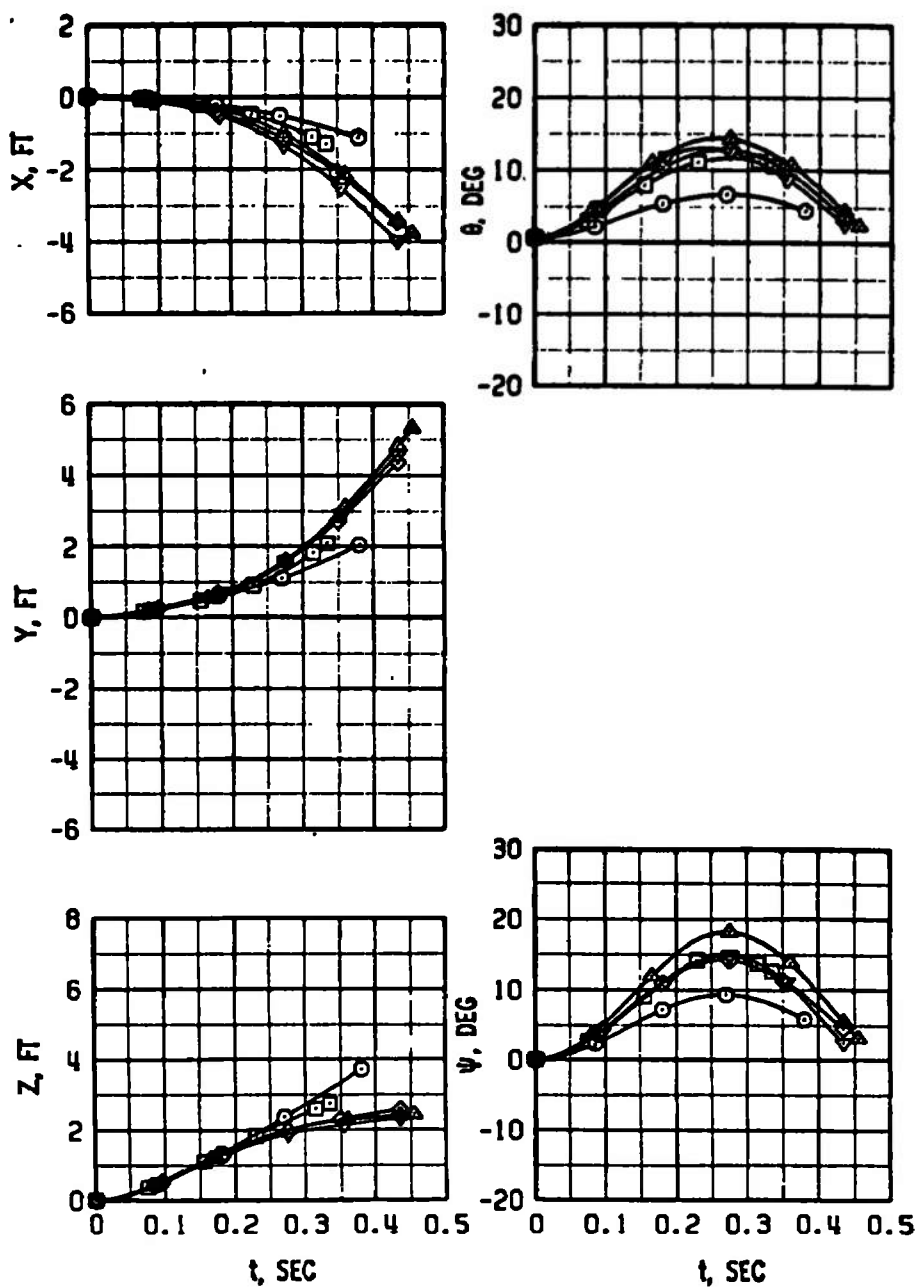
d. Configuration 6, pylon 6
Figure 12. Continued.

SYM	M_∞	α	A_E	PYLON	BAU	STA	CONF
○	0.90	2	54	3	6	7	
□	0.95	2	54	3	6	7	
△	0.97	2	54	3	6	7	
◇	1.02	2	54	3	6	7	
▽	1.05	2	54	3	6	7	



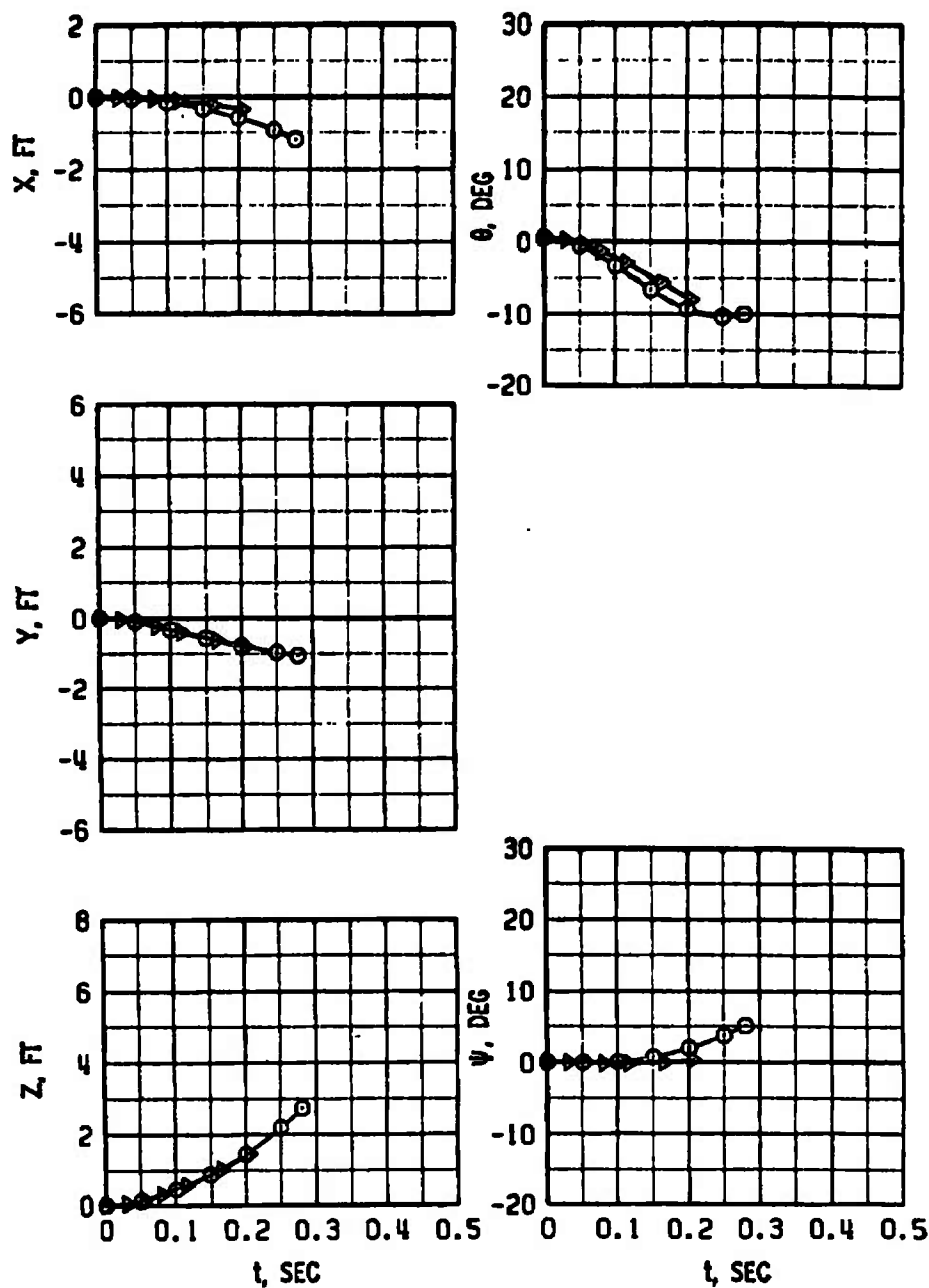
e. Configuration 7, pylon 3
Figure 12. Continued.

SYM	M_∞	α	A_{LE}	PYLON	BRU	STA	CONF
○	0.90	2	54	6	6	7	
□	0.95	2	54	6	6	7	
▲	0.97	2	54	6	6	7	
◇	1.02	2	54	6	6	7	
▼	1.05	2	54	6	6	7	



f. Configuration 7, pylon 6
Figure 12. Concluded.

SYM	M_∞	α	Λ_L	PYLON	BAU STA	CONF	H
○	1.05	2	54	3	3	4	1,000
▶	1.05	3	54	3	3	4	15,000



a. $M_\infty = 1.05$, pylon 3, configuration 4

Figure 13. Typical effect of altitude variation on the MK-82 AIR trajectories.

SYM	M_∞	α	Λ_{LE}	PYLON	BRU	STA	CONF	H
○	0.95	3	60	6	4	11	1,000	
□	0.95	3	60	6	4	11	15,000	

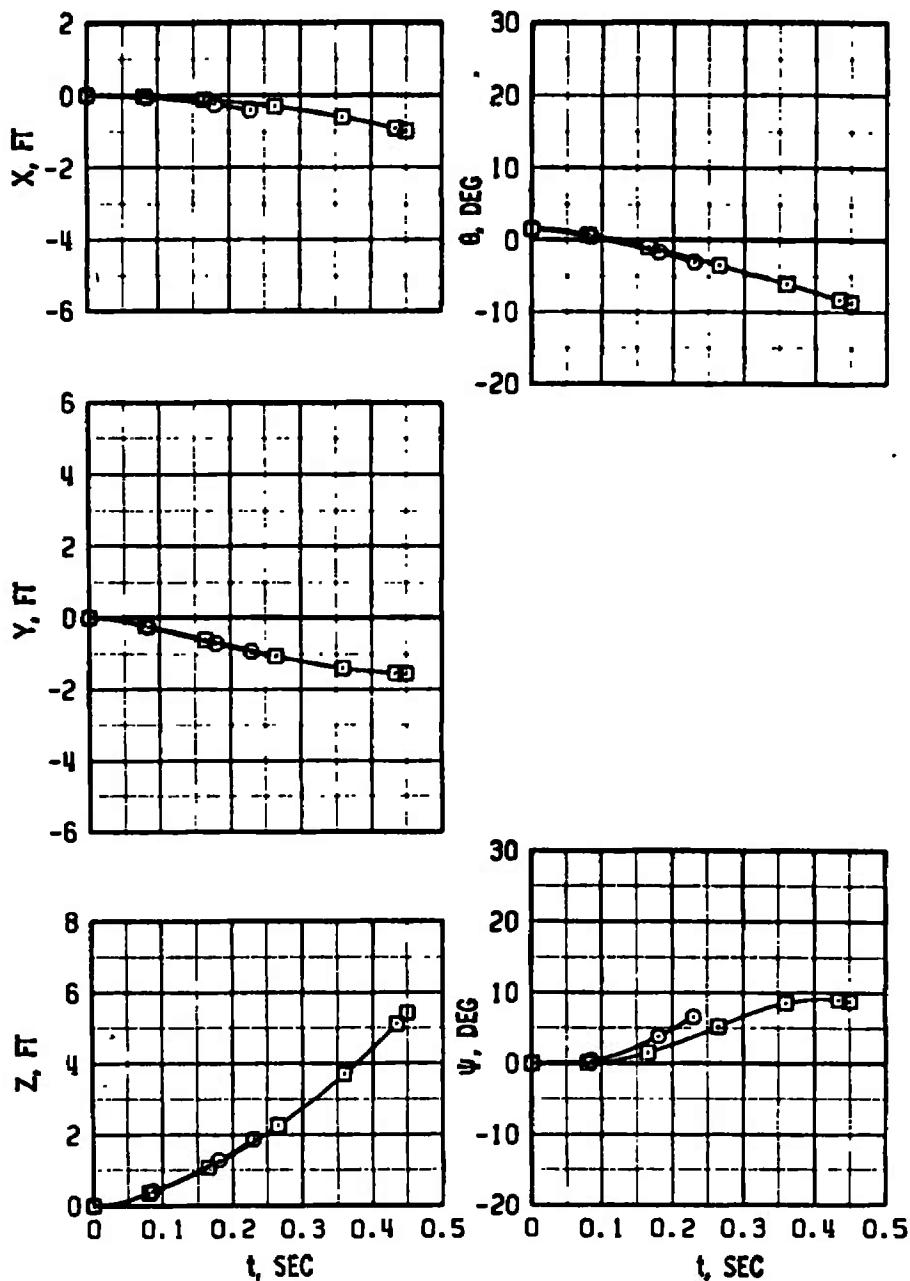
b. $M_\infty = 0.95$, pylon 6, configuration 11

Figure 13. Concluded.

Table 1. Wind Tunnel Nominal Test Conditions





M_∞	p_t , psfa	T_t , °R	p_∞ , psfa	q_∞ , psf	$Re_\infty \times 10^{-6}$, ft ⁻¹
0.70	1,800	540	1,300	440	3.4
0.80	1,800		1,180	530	3.6
0.90	1,400		830	470	3.0
0.95			780	490	2.8
0.97			765	500	2.8
1.02			720	525	2.9
1.05	1,200		600	460	2.5
1.15			530	490	
1.25			460	510	

Table 2. Test Summary

Config	M _∞	Release Station		α, deg	λ _{LE} , deg	Altitude, ft	Ejector* Force
		Pylon	BRU				
1 ↓ ↓							

*See Table 3b.

Table 2. Continued

Config	M_∞	Release Station		α , deg	λ_{LE} , deg	Altitude, ft	Ejector* Force
		Pylon	BRU				
3	1.05	6	2	2	60	1,000	E-1
	1.15						
	1.25						
	1.05			3	72.5		
	1.15						
	1.25						
4	0.9	3	3	2	54		
	0.9	6	4				
	0.95	6	4				
		3	3				
		3	3	3		15,000	
	0.97	6	4	2		1,000	
	0.97	3	3				
	1.02	3	3				
	1.02	6	4				
	1.05	3	3				
	1.05	3	3			15,000	
						1,000	
	0.95	6	3				
	0.95	3	4				
5	1.05	3	4				
	1.05	6	3				
	0.9	3	5				
	0.9	6					
6	0.95	6					
	0.95	3					
	0.97	3					
	0.97	6					
	1.02	6					
		3					
	1.05						

*See Table 3b.

Table 2. Continued

Config	M_∞	Release Station		α , deg	λ_{LE} , deg	Altitude, ft	Ejector* Force
		Pylon	BRU				
6	1.05	6	5	2	54	1,000	E-1
7	0.9	3	6				
	0.9	6					
	0.95	6					
	0.95	3					
	0.97	3					
	0.97	6					
	1.02	6					
	1.02	3					
	1.05	3					
	1.05	6					
8	0.95	6	5		60		
	0.95	3	3				
	1.05	3	3				
	1.05	6	5				
	1.15	3	3				
	1.25	3	3				
	1.25	6	5				
	1.05	3	3				
	1.05	6	5				
	1.15	6	5				
	1.15	3	3				
	1.25	3	3				
	1.25	6	5				
	1.05	3	4				
	1.05	6	6				
	1.15						
9	1.25	3	4				E-2
	1.25						E-1
	1.25						
	1.25						E-2

*See Table 3b.

Table 2. Continued

Config	M_∞	Release Station		α , deg	λ_{LE} , deg	Altitude, ft	Ejector* Force
		Pylon	BRU				
9 ↓ 10	1.25	6	6	3	72.5	1,000	E-1
	0.95	3	4	2	60		
	↓	6	6	2	↓		
	1.05	↓	↓	3			
	1.05	3	4	2			
	1.15	3	4	↓			
	1.15	6	6				
	1.25	6	6				
	0.95	3	5	↓			
	↓	6	3	3			
10 ↓ 11	0.95	6	3	↓			
	↓	6	3	3			
	↓	3	5	↓			
	↓	3	5	↓		15,000	
	1.05	6	3	2		1,000	
	1.05	3	5	↓			
	1.15	3	5	↓			
	1.15	6	3	↓			
	1.05	3	5	3	72.5		
	1.05	6	3	↓			
	1.15	6	3	↓			
	1.15	3	5	↓			
	1.25	3	5	↓			
	1.25	6	3	↓			
	0.9	3	5	2	54		
	0.9	6	3	↓			
	0.95	6	3	↓			
	0.95	3	5	↓			
	1.05	3	5	↓			
	1.05	6	3	↓			
	0.9	3	6	↓			

*See Table 3b.

Table 2. Concluded

Config	M_∞	Release Station		α , deg	λ_{LE} , deg	Altitude, ft	Ejector* Force
		Pylon	BRU				
11	0.9	6	4	2	54	1,000	E-1
	0.95	6	4				
	0.95	3	6				
	0.97	3	6				
	0.97	6	4				
	1.02	6	4				
	1.02	3	6				
	1.05	3	6				
	1.05	6	4				
	0.95	3	6		60		
		6	4				
				3			
						15,000	
		3	6			1,000	
	1.05	3	6	2			
	1.05	6	4				
	1.15	6	4				
	1.15	3	6				
	1.25	6	4				
	1.05	3	6	3	72.5		
	1.05	6	4				
	1.15	6	4				
	1.15	3	6				
	1.25	6	4				

*See Table 3b.

Table 3. Input Constants Used in Trajectory Calculations
a. Full Scale Store Parameters

Symbol	Parameter	Value
S	Store Reference Area, ft ²	0.630
B	Store Reference Dimension, ft	0.896
I _{xx}	Moment of Inertia, slug-ft ²	1.380
I _{yy}	Moment of Inertia, slug-ft ²	45.740
I _{zz}	Moment of Inertia, slug-ft ²	45.740
C _{m_q}	Pitch-Damping Derivative, per radian	-150.0
C _{n_r}	Yaw-Damping Derivative, per radian	-150.0
C _{l_p}	Roll-Damping Derivative, per radian	-2.0
X _{cg}	Center-of-Gravity Location from Nose, ft	3.222
Z _{cg}	Center-of-Gravity Location Above Centerline, ft	0
\bar{m}	Mass, slugs	16.318
X _{L₁}	Forward Ejector Piston Location, ft	0.621
X _{L₂}	Aft Ejector Piston Location, ft	-0.546
Z _E	Ejector Stroke Length, ft	0.250

Table 3. Concluded
b. Ejector Force

Designation	F_{Z_1} , lb	F_{Z_2} , lb
E-1	1,000	800
E-2	1,800	0
E-3	0	1,200

c. Axial-Force Coefficient

M_∞	C_A
0.7	0.28
0.8	0.28
0.9	0.30
0.95	0.33
0.97	0.36
1.02	0.43
1.05	0.47
1.15	0.50
1.25	0.50

NOMENCLATURE

BL	Aircraft buttock line from plane of symmetry, in., model scale
b	Store reference dimension, ft, full scale
C_A	Store axial-force coefficient, axial force/ $q_\infty S$
C_ℓ	Store rolling-moment coefficient, rolling moment/ $q_\infty S b$
C_{ℓ_p}	Roll-damping derivative, per radian
C_m	Store pitching-moment coefficient, referenced to the store cg, pitching moment/ $q_\infty S b$
C_{m_q}	Store pitch-damping derivative, $dC_m/d(qb/2V_\infty)$
C_N	Store normal-force coefficient, normal force/ $q_\infty S$
C_n	Store yawing-moment coefficient, referenced to the store cg, yawing moment/ $q_\infty S b$
C_{n_r}	Store yaw-damping derivative, $dC_n/d(rb/2V_\infty)$
C_Y	Store side-force coefficient, side force/ $q_\infty S$
F_{Z_1}	Forward ejector force, lb
F_{Z_2}	Aft ejector force, lb
H	Simulated altitude, ft, full scale
I_{xx}	Full-scale moment of inertia about the store X_B axis, slug-ft ²
I_{yy}	Full-scale moment of inertia about the store Y_B axis, slug-ft ²
I_{zz}	Full-scale moment of inertia about the store Z_B axis, slug-ft ²
M_∞	Free-stream Mach number
\bar{m}_∞	Full-scale store mass, slugs
p_t	Free-stream total pressure, psfa
p_∞	Free-stream static pressure, psfa

q	Store angular velocity about the Y_B axis, radians/sec
q_∞	Free-stream dynamic pressure, psf
Re_∞	Free-stream unit Reynolds number, per ft
r	Store angular velocity about the Z_B axis, radians/sec
S	Store reference area, ft^2 , full scale
T_t	Free-stream total temperature, $^\circ R$
t	Real trajectory time from initiation of trajectory, sec
V_∞	Free-stream velocity, ft/sec
X	Separation distance of the store cg parallel to the flight axis system X_F direction, ft, full scale measured from the prelaunch position
X_{cg}	Full-scale cg location, ft from nose of store
X_{L1}	Forward ejector location relative to the store cg, positive forward of store cg, ft, full scale
X_{L2}	Aft ejector piston location relative to the store cg, positive forward of store cg, ft, full scale
Y	Separation distance of the store cg parallel to the flight axis system Y_F direction, ft, full scale measured from the prelaunch position
Z	Separation distance of the store cg parallel to the flight axis system Z_F direction, ft, full scale measured from the prelaunch position
Z_{cg}	Full-scale cg location, ft above centerline of store
Z_E	Ejector stroke, ft
α	Aircraft model angle of attack relative to the free-stream velocity vector, deg
θ	Angle between the store longitudinal axis and its projection in the X_F - Y_F plane, positive when store nose is raised as seen by pilot, deg

Λ_{LE}	Parent-aircraft wing leading edge sweep angle, deg
ψ	Angle between the projection of the store longitudinal axis in the X_F - Y_F axis, positive when the store nose is to the right as seen by the pilot, deg

FLIGHT AXIS SYSTEM COORDINATES

Directions

X_F	Parallel to the free-stream wind vector, positive direction is forward as seen by the pilot
Y_F	Perpendicular to the X_F and Z_F directions, positive direction is to the right as seen by the pilot
Z_F	In the aircraft plane of symmetry, perpendicular to the free-stream wind vector, positive direction is downward

The flight axis system origin is coincident with the aircraft cg and remains fixed with respect to the parent aircraft during store separation. The X_F , Y_F , and Z_F coordinate axes do not rotate with respect to the initial flight direction and attitude.

STORE BODY AXIS SYSTEM COORDINATES

Directions

X_B	Parallel to the store longitudinal axis, positive direction is upstream in the prelaunch position
Y_B	Perpendicular to the store longitudinal axis, and parallel to the flight axis system X_F - Y_F plane when the store is at zero roll angle, positive direction is to the right looking upstream when the store is at zero yaw and roll angles
Z_B	Perpendicular to both the X_B and Y_B axes, positive direction is downward as seen by the pilot when the store is at zero pitch and roll angles.

The store body axis system origin is coincident with the store cg and moves with the store during separation from the parent airplane. The X_B , Y_B , and Z_B coordinate axes rotate with the store in pitch, yaw, and roll so that mass moments of inertia about the three axes are not time-varying quantities.